We are IntechOpen,
the world's leading publisher of
Open Access books
Built by scientists, for scientists

4,800
Open access books available

122,000
International authors and editors

135M
Downloads

Our authors are among the

154
Countries delivered to

TOP 1%
most cited scientists

12.2%
Contributors from top 500 universities

BOOK CITATION INDEX
CLARIVATE ANALYTICS
INDEXED

WEB OF SCIENCE™

Selection of our books indexed in the Book Citation Index
in Web of Science™ Core Collection (BKCI)

Interested in publishing with us?
Contact book.department@intechopen.com

Numbers displayed above are based on latest data collected.
For more information visit www.intechopen.com

Dielectric Screening Properties and Many Body Effects in Molten Salts

Shigeki Matsunaga[1], Takahiro Koishi[2],
Masatoshi Saito[3] and Shigeru Tamaki[3]
[1]Nagaoka National College of Technology
[2]University of Fukui Graduate School of Engineering
[3]Niigata University
Japan

1. Introduction

The dielectric screening properties in molten salts have been a matter of particular interest. There is a close relation between the dielectric screening and the charge fluctuation of the constituents of the substances. The charge-charge structure factor, or $S_{ZZ}(q)$ (Hansen & McDonald, 1986), indicates the charge fluctuation in a molten salt, which can be easily obtained by the linear transformation from their partial structure factors. The dielectric screening function, or $\varepsilon(q)$, of a mono-valent molten salt has been represented by $S_{ZZ}(q)$ as follows,

$$1 / \varepsilon(q) = 1 - \{4\pi e^2 \beta n\, S_{ZZ}(q) / q^2\} \tag{1}$$

where $\beta = 1/k_B T$ and n is the number density of constituent ions (Hansen & McDonald, 1986).

On the other hand, the partial structure factors of various molten salts have been experimentally obtained by applying a combination of different diffraction methods, *e.g.* X-ray and neutron diffraction, to the same molten salts. Therefore, $S_{ZZ}(q)$ of molten salts are obtainable by experiment from their partial structure factors (Saito et al, 1999). Several attempts have been made at deriving the dielectric screening functions from the experimental structure factors and Eq. (1). However, the obtained results indicate a *negative* sign in the small q region. This fact shows the difficulty in the appropriate explanation of the results, because $\varepsilon(q)$ should be *positive* in the meaning of the potential screening. In this situation, we have proposed the *new* equation of $\varepsilon(q)$ and $S_{ZZ}(q)$ in molten salts which formula is different from Eq.(1). In order to test the new theory, we have applied it to molten alkali-halides (Koishi et al, 2007) and noble metal halides and their mixtures (Matsunaga et al, 2007, 2008, 2011).

In this book chapter, firstly, we summarize the re-examination of the theory, and the derivation of the alternative expression of the dielectric function. Then, we wish to show the application of the theory to the molten salts; alkali halides NaCl, RbBr, noble metal halides AgBr, CuBr, and mixture AgBr-AgI. AgBr-CuBr system will be treated in the

context of the many body effect. The extension of the theory to the polarizable ion model will also been discussed with the application to CuI and CsAu melt.

2. Theoretical background of dielectric screening

The theory of the dielectric screening effect in molten salt has been re-examined in relation with the charge-charge structure factor in our previous work (Koishi et al, 2007; Matsunaga et al, 2007, 2008, 2011). In this chapter, for the readers' benefit, we summarize the theoretical back ground of the charge-charge structure factor firstly, then the derivation of the new expression of the dielectric function in relation with the dielectric screening.

2.1 Charge-charge structure factors in molten salts

We consider a typical binary molten salt system $A_\nu B_\mu$. N_ν and N_μ stand for the number of ion species + and -. With the total number of particles N, the concentration of species ν is expressed as $x_\nu = N_\nu/N = 0.5$. The densities of particles are $n^\nu = n^\mu = n^0 = n/2$ and $n = N/V$, where V is the volume of the system. The effective charges of ions are $|z^\nu| = |z^\mu| = z$. The charge-charge structure factor, $S_{ZZ}(q)$, defined by Hansen-McDonald is useful representation for charged fluid, which is written as follows (Hansen & McDonald, 1986),

$$S_{zz}(q) = <\rho_q^z \rho_q^z> /N = \Sigma_\nu \Sigma_\mu z_\nu z_\mu S_{\nu\mu}(q) \tag{2}$$

where $S_{\nu\mu}(q)$ is a partial structure factor, *i.e.* the Fourier transformation of the pair distribution function of ion ν around ion μ in r-space, $g_{\nu\mu}(r)$. $S_{\nu\mu}(q)$ is defined as,

$$S_{\nu\mu}(q) = x_\nu \delta_{\nu\mu} + nx_\nu x_\mu \int_0^\infty (\sin qr / qr)\{(g_{\nu\mu}(r) - 1)\} 4r^2 dr \tag{3}$$

$S_{\nu\mu}(q)$ and $g_{\nu\mu}(r)$ directly reflect the ionic configuration and are easily obtainable from neutron diffraction experiment or molecular dynamics simulation.

Using $g_{\nu\mu}(r)$ ($\nu,\mu = +,-$), $S_{zz}(q)$ is given by,

$$S_{zz}(q) = 1 + (n/2)\int_0^\infty (\sin qr / qr)\{(g_{++}(r) - 1) + (g_{--}(r) - 1) - 2(g_{+-}(r) - 1)\} 4\pi r^2 dr \tag{4}$$

On the other hand, the concentration-concentration fluctuation in r-space $g_{cc}(r)$ defined by Bhatia-Thornton representation is written as follow (Bhatia & Thornton, 1970),

$$\begin{aligned} g_{cc}(r) &= x_\nu^2 x_\mu^2 [(g_{++}(r) - 1) + (g_{--}(r) - 1) - 2(g_{+-}(r) - 1)] \\ &= (1/16)\left[(g_{++}(r) - 1) + (g_{--}(r) - 1) - 2(g_{+-}(r) - 1)\right] \end{aligned} \tag{5}$$

Corresponding to $g_{cc}(r)$, the concentration-concentration structure factor $S_{cc}(q)$ is defined as follows,

$$\begin{aligned} S_{cc}(q) &= x_\nu x_\mu + n\int_0^\infty (\sin qr / qr) g_{cc}(r) 4\pi r^2 dr \\ &= 1/4 + n\int_0^\infty (\sin qr / qr) g_{cc}(r) 4\pi r^2 dr \end{aligned} \tag{6}$$

Inserting (5) into (6) and using (4), we have,

$$S_{zz}(q) = 4\,S_{cc}(q) \tag{7}$$

Using the formulae obtained in this section, the dielectric screening functions in terms of $S_{zz}(q)$ will be shown in the next section.

2.2 Dielectric screening function expressed in terms of $S_{zz}(q)$

In order to derive the dielectric screening function, we will consider the same molten salt system considered in the preceding section. If a charge $e\rho_{ext}(\mathbf{r})$ were introduced from outside into this system at the position $\mathbf{r}$, then there occurs an induced charge $e\rho_{ind}(\mathbf{r})$ at its position. Therefore we have the following Poisson equations in the electrostatic unit,

$$\mathrm{div}\boldsymbol{D}(\mathbf{r}) = 4\pi e\rho_{ext}(\mathbf{r}) \tag{8}$$

$$\mathrm{div}\boldsymbol{E}(\mathbf{r}) = 4\pi e\{\rho_{ext}(\mathbf{r}) + \rho_{ind}(\mathbf{r})\} \tag{9}$$

where $\boldsymbol{D}(\mathbf{r})$ and $\boldsymbol{E}(\mathbf{r})$ the electric displacement and the electric field, respectively.

The electric potential $\varphi(\mathbf{r})$ due to this external charge density is given by

$$E(\mathbf{r}) = -\mathrm{grad}\varphi(\mathbf{r}) \tag{10}$$

Using (9) we have

$$\nabla^2\varphi(\mathbf{r}) = -\{4\pi e\rho_{ext}(\mathbf{r})/\varepsilon\} \tag{11}$$

$$= -4\pi e\{\rho_{ext}(\mathbf{r}) + \rho_{ind}(\mathbf{r})\} = -4\pi e\rho_{ext}(\mathbf{r})\big[1 + \{\rho_{ind}(\mathbf{r})/\rho_{ext}(\mathbf{r})\}\big] \tag{12}$$

where ε is the dielectric constant, but it may be extended to an isotropic r-dependent term written as $\varepsilon(r)$.

In their text book, Hansen and McDonald took partly $\varepsilon(r) = 1$ for the dielectric function in molten salts and obtained the formula expressed as shown in Eq. (1).

Now we can express each quantity $\varepsilon(\mathbf{r})$, $\varphi(\mathbf{r})$ and $\rho_{ext}(\mathbf{r})$ in this equation as the following Fourier representations,

$$\varepsilon(\mathbf{r}) = \sum_q \underline{\varepsilon}(\mathbf{q})e^{i\mathbf{q}\cdot\mathbf{r}}, \ \varphi(\mathbf{r}) = \sum_q \underline{\varphi}(\mathbf{q})e^{i\mathbf{q}\cdot\mathbf{r}}, \ \rho_{ext}(\mathbf{r}) = \sum_q \underline{\rho}_{ext}(\mathbf{q})e^{i\mathbf{q}\cdot\mathbf{r}}$$

and
$$\rho_{ind}(\mathbf{r}) = \sum_q \underline{\rho}_{ind}(\mathbf{q})e^{i\mathbf{q}\cdot\mathbf{r}} \tag{13}$$

Putting some of these into equation (11) and taking $\mathbf{r} = 0$, we have

$$q^2\varepsilon(q)\underline{\varphi}(\mathbf{q}) = 4\pi e\underline{\rho}_{ext}(\mathbf{q}) \tag{14}$$

where $\underline{A}(\mathbf{q}) = \{A_x(\mathbf{q}), A_y(\mathbf{q}), A_z(\mathbf{q})\}$. And we assume that $\underline{\varepsilon}(\mathbf{q})$ is isotropic, which is expressed as $\varepsilon(q)$.

Since $e\rho_{ind}(\mathbf{r})$ is a charge fluctuation by the insertion of the external charge $e\rho_{ext}(\mathbf{r})$, it might be expressed in the following form, by using the linear charge response function $\chi_{zz}(q)$,

$$\underline{\rho}_{ind}(\mathbf{q}) = \chi_{zz}(q)e\underline{\varphi}(\mathbf{q}) \tag{15}$$

Based on the fluctuation dissipation theorem, $\chi_{zz}(q)$ is expressed in terms of $S_{zz}(q)$ as follows,

$$\chi_{zz}(q) = -\beta n S_{zz}(q) \tag{16}$$

Compare equations (11) and (12), the inverse dielectric function $1/\varepsilon(q)$ is expressed as follows,

$$1/\varepsilon(q) = FT\{\mathrm{div}E(\mathbf{r})\} / FT\{\mathrm{div}D(\mathbf{r})\} = \{\mathbf{q}\cdot\underline{E}(q)\} / \{\mathbf{q}\cdot\underline{D}(q)\} = 1 + \{\underline{\rho}_{ind}(\mathbf{q}) / \underline{\rho}_{ext}(\mathbf{q})\} \tag{17}$$

where FT means the Fourier component.

Putting (14) and (15) into (17), and using (16), we have

$$1/\varepsilon(q) = 1 + \{4\pi e^2 \chi_{zz}(q) / \varepsilon(q)q^2\} = 1 - \{4\pi e^2 \beta n S_{zz}(q) / \varepsilon(q)q^2\} \tag{18}$$

or

$$1/\varepsilon(q) = 1 / \{1 + (\kappa_s^2 / q^2)S_{zz}(q)\} \tag{19-a}$$

where

$$\kappa_s^2 = 4\pi e^2 \beta n \tag{19-b}$$

Equation (19-a) is resulted from an isotropic configuration of surrounded ions, which condition can be satisfied by a symmetric configuration in the short range region in the molten salt that consists of almost perfectly ionized ions such as in molten NaCl and CsCl. If the ions' configuration deviates extremely from an isotropic one, which can be, for instance, seen in molten CuI in which the oscillation of $g^{Cu-I}(r)$ for the distance r coincides basically with that of $g^{Cu-Cu}(r)$ (Waseda et al.,2000), then the dielectric screening may include some anisotropic effect and the application of equation (19-a) becomes insufficient. We will discuss this point in the later section. A rather simplified revision for such a case is the insertion of a parameter δ into equation (19-a) defined as,

$$1/\varepsilon(q) = 1 / \{1 + \delta(\kappa_s^2 / q^2)S_{zz}(q)\} \tag{20}$$

Magnitude of δ may be in the range of $0 < \delta \leq 1$ and the condition $\delta = 1$ may occur in a well symmetric configuration. In the region of higher values of $q > 10A^{-1}$, we have usually $S_{zz}(q) \simeq 1$ and then

$$1/\varepsilon(q) = 1 / \{1 + \delta(\kappa_s^2 / q^2)\} \tag{21}$$

On the other hand, the inverse dielectric function in the long wavelength limit is already well known by the theory of classical one component plasma (Hansen & McDonald, 1986; March & Tosi, 1976). Starting from the continuity equation relating to the charge and taking Fourier transforms under the condition of long wavelength limit, the relation between $\rho_{ind}(q)$ and $\rho_{ext}(q)$ is expressed as follows,

$$\rho_{ind}(q) = -\rho_{ext}(q) / \left\{ 1 + \left(q^2 / \lambda_s^2 \right) \right\} \tag{22}$$

where

$$\lambda_s^2 = 4\pi e^2 n^2 \chi_T \tag{23}$$

here χ_T being the isothermal compressibility and $n = 2n_0 = n^+ + n^-$. If an external point charge ze is put at the position r, then we have the well-known Thomas-Fermi type screening potential by using equation (22), which indicates that the inverse dielectric function near the long wavelength limit is written as follows,

$$1 / \varepsilon(q) = 1 / \left\{ 1 + \left(\lambda_s^2 / q^2 \right) \right\} \tag{24}$$

It is interesting that the inverse dielectric function $1/\varepsilon(q)$ in its higher q-region and very lower q-region is expressed by a similar form as shown in equations (21) and (24), although their screening constants are quite different. In the intermediate region, $1/\varepsilon(q)$ exhibits an oscillating behavior due to the effect of $S_{zz}(q)$, as a logical consequence.

Using (6) and (7), $S_{zz}(q)$ is given by

$$S_{zz}(q) = \sum_v \sum_\mu z_v z_\mu S_{v\mu}(q) = 1 + 8n \int_0^\infty \frac{\sin qr}{qr} g_{cc}(r) 4\pi r^2 dr \tag{25}$$

where we took that the ionic charges are equal to the ionic valences as $z^+ = -z^- = z = 1$. Therefore $1/\varepsilon(q)$ is converted to

$$\frac{1}{\varepsilon(q)} = \frac{1}{1 + \delta\left(\kappa_s^2 / q^2 \right) \{ 1 + 8n \int_0^\infty (\sin qr / qr) g_{cc}(r) 4\pi r^2 dr \}} \tag{26}$$

Under the assumption of $\delta = 1$, equation (19) is useful for deriving the inverse dielectric function, $1/\varepsilon(q)$, from experimental results for the partial structure factors and also equation (25) is applicable for deriving $1/\varepsilon(q)$ by a computer simulation.

It is apparent that equation (24) is equal to zero at $q=0$. And therefore, the inverse dielectric function $1/\varepsilon(q)$ has the following relation for any positive values of $S_{zz}(q)$,

$$0 \leqq 1 / \varepsilon(q) \leqq 1 \tag{27}$$

At this point, it should be stressed that the validity of Eq.(20) and Eq.(21) is also confirmed by this fact in the meaning of screening; $1/\varepsilon(q)$ remains *positive* for all positive q value. It is therefore possible to derive the inverse dielectric function $1/\varepsilon(q)$ if $S_{zz}(q)$ or

$g_{cc}(r)$ are known by either the experimental method or computer simulation under the assumption of $\delta = 1$. In the following sections we will show several results for $1/\varepsilon(q)$ by using experimental $S_{zz}(q)$ and simulated $g_{cc}(r)$.

2.3 Screening for Coulomb potential in a molten salt

In a molten salt having the charges of $z^+ = -z^- = 1$, the screened potential between a cation and an anion, $\varphi^{+-}_{sc}(r)$, may be divided into two parts as follows,

$$\varphi^{+-}_{sc}(r) = \varphi^{+-}_{sc\,rep}(r) + \varphi^{+-}_{sc\,at}(r) \tag{28}$$

Here $\varphi^{+-}_{sc\,rep}(r)$ is the repulsive potential influenced by a small amount of screening effect in the short range distance between cation and anion, and $\varphi^{+-}_{sc\,at}(r)$ is the attractive screened potential in the long range.

The utilization of equation (19-a) for the repulsive potential seems not to be a good and enough approximation as the screening effect, because the application of linear response theory for a highly nonlinear functional form cannot give any good approximation. Therefore, equation (16) is a poor approximation for the repulsive potential because of its highly nonlinear functional form, and therefore the screening effect for the direct repulsive potential should be treated in a different way. A simple consideration for the screening effect for the repulsive potential is the introduction of parametric multiplier, hereafter taken as α, which can be multiplied to the well-known formula of the repulsive potential as a multiplicand. Then the screened repulsive potential may be written as follows,

$$\varphi^{+-}_{sc\,rep}(r) = \alpha \varphi^{+-}_{rep}(r) \tag{29}$$

where $\varphi^{+-}_{rep}(r)$ is the bare repulsive potential. On the other hand, the attractive screened potential $\varphi^{+-}_{sc\,at}(r)$ is effectively screened by the existence of other ions, although its bare-potential may be mainly ascribed to the form of Coulomb interacting potential. Let put an ion of positive point charge at the origin. Then another ion of negative point charge in the region of attractive Coulomb potential at r feels the following potential,

$$\varphi^{+-}_{at}(r) = -e^2 / r \tag{30}$$

Therefore, the screened attractive potential in q-space is written as follows,

$$\varphi^{+-}_{sc\,at}(q) = -4\pi e^2 / \varepsilon(q)q^2 \tag{31}$$

The numerical result for $\varphi^{+-}_{sc\,at}(r)$ is given by the inverse Fourier transformation FT$\{\varphi^{+-}_{sc\,at}(q)\}$. The repulsive potential $\varphi^{+-}_{rep}(r)$ which is often approximated by either the Born-Mayer type potential or the inverse function of r^n ($n \leq 12$). That is,

$$\varphi^{+-}_{rep}(r) = A \cdot \exp(-br) \qquad \text{or} \qquad \varphi^{+-}_{rep}(r) = B / r^n \qquad (n \leq 12) \tag{32}$$

where A, b, B and n are constants. Equation (28) is therefore converted to

$$\varphi^{+-}_{sc}(r) = \alpha\, A \exp(-br) + FT\left\{\varphi^{+-}_{sc\,at}(q)\right\} \tag{33-a}$$

or

$$\varphi^{+-}_{sc}(r) = \alpha\left(B/r^n\right) + FT\left\{\varphi^{+-}_{scat}(q)\right\} \tag{33-b}$$

In the region of $S_{zz}(q)\sim1$, equation (21) is applicable. If $\delta=1$, then we have,

$$\varphi^{+-}_{scat}(q) = -\left(4\pi e^2/q^2\right)\left\{q^2/\left(q^2+\kappa_s^2\right)\right\} = -4\pi e^2/\left(q^2+\kappa_s^2\right) \tag{34}$$

This equation is easily converted to the r-dependent expression as

$$\varphi^{+-}_{scat}(r) = -\left(e^2/r\right)\exp(-\kappa_s r) \tag{35}$$

The screening parameter κ_s is exactly equal to the inverse of the Debye screening length. Using (32) and (35), the effective potential of mean force between cation and anion in the region of $S_{zz}(q)\sim1$ is then expressed as,

$$\varphi^{+-}_{sc}(r) = \alpha\, A\cdot\exp(-br) - \left(e^2/r\right)\exp(-\kappa_s r) \tag{36-a}$$

or

$$\varphi^{+-}_{sc}(r) = \alpha\, B/r^n - \left(e^2/r\right)\exp(-\kappa_s r) \tag{36-b}$$

It is emphasized that the inverse dielectric function $1/\varepsilon(q)$ as the screening effect can be multiplied onto the bare attractive inter-ionic potential between two ions in the q-space, and the screening parameter α is also multiplied onto the repulsive potential in r-space, in order to obtain the effective screened potential

2.4 Equivalency between the screened pair potential and the potential of mean force

We have obtained an asymptotic form for the screened attractive potential, as shown in Eq. (35). The factor $\exp(-\kappa_s r)$ is familiar in the elementary Debye-Hückel theory and the corresponding pair distribution function $g_{+-}(r)$ is given by,

$$g_{+-}(r) = \exp\{\frac{\beta e^2}{r}\exp(-\kappa_s r)\} \tag{37}$$

In this section, we will prove that this asymptotic form of the screened attractive potential $\varphi^{+-}_{scat}(r)$ and the potential of mean force $U^{+-}(r)$ defined by the formula of

$$g_{+-}(r) = \exp\left\{-U^{+-}(r)/k_B T\right\} \tag{37-a}$$

are equal to each other at the long distance of r, by using the Ornstein-Zernike equation. Putting a cation 1 at the origin and an anion 2 at the position r, and furthermore the third ion 3 at the position r', then we have an approximate Ornstein-Zernike equation as follows,

$$-\beta U^{+-}(r) = -\beta\varphi^{+-}(r) + n\int dr\, c_{+-}(|r-r'|)h_{--}(r') \tag{38}$$

where $c_{+-}(r)$ is the direct correlation function between cation and anion, and $h_{--}(r')$ is equal to $(g_{--}(r') - 1)$. Hence we have inferred that the third ion represented by 3 is mainly another neighboring anion located around the cation at the origin, because the ion 3 is located at a

closer position to the origin, which means that its sign is negative. By Fourier transformation, Eq.(38) is converted to the following form,

$$U^{+-}(q) = \varphi^{+-}(q)\left[1 - \frac{c_{+-}(q)h_{--}(q)}{\beta n \varphi^{+-}(q)}\right] \tag{39}$$

On the other hand, it is well known that the direct correlation function $c_{+-}(r)$ has a approximate form for large r, as follows,

$$c_{+-}(r) \cong -\beta \varphi^{+-}(r) \tag{40}$$

The Fourier transformation of Eq.(40) is immediately written as,

$$c_{+-}(q) \cong -n\beta \varphi^{+-}(q) \tag{41}$$

Putting (41) into (39), we have

$$U^{+-}(q) \cong \varphi^{+-}(q)\{1 + h_{--}(q)\} = \varphi^{+-}(q)S_{--}(q) \tag{42}$$

Apart from a quantitative disagreement with either the experimental result or simulated one, $S_{--}(q)$ may be analogically expressed as follows, by using the random phase approximation (March and Tosi, 1976),

$$S_{--}(q) = \frac{1}{1+n\beta\varphi^{--}(q)} \tag{43}$$

Here the pair potential between anions in its Fourier transformation $\varphi^{--}(q)$ is also approximately expressed as $4\pi e^2/q^2$, and then we have,

$$U^{+-}(q) = -\frac{4\pi e^2}{q^2 + \kappa_s^2} \tag{44}$$

And finally we have,

$$U^{+-}(q) = -\frac{e^2}{r}\exp(-\kappa_s r) \tag{45}$$

Therefore, $\varphi^{+-}_{sc\ at}(r)$ described in Eq. (35) and the potential mean force $U^{+-}(r)$ are equal to each other at the long distance of r. The expression of $\varphi^{+-}_{sc\ at}(r)$ is certainly not rigorous, and therefore there is inevitably a minor discrepancy between $\varphi^{+-}_{sc\ at}(r)$ and $U^{+-}(r)$ in the numerical agreement. However, in an approximate sense, both functions are equivalent. In fact, the screened potential between the centered cation 1 and neighboring anion 2 locating at an appropriate distance, is expressed in terms of the form of direct interacting potential multiplied by the inverse dielectric function $1/\varepsilon(q)$. The factor $1/\varepsilon(q)$ is evidently given by the force acting on the centered cation from all other neighboring ions represented by 3. Therefore, the screened potential is physically equivalent to the potential of mean force.

2.5 Deviation from Nernst-Einstein relation

In this section, we wish to deal with a practical application of the potential of mean force $U^{+-}(r)$ in molten salts. The deviation, Δ, from the Nernst-Einstein relation in nomovalent molten salts is defined as follows,

$$\sigma = \sigma^+ + \sigma^- = \left(ne^2 / k_B T\right)\left(D^+ + D^-\right)(1 - \Delta) \tag{46}$$

The partial conductivities for cation and anion, σ^+ and σ^-, and the diffusion constants D^+ and D^- were already derived before (Koishi & Tamaki, 2005). Taking these results, we have

$$\Delta = 1 - \left(1 - \Delta_{BR}\right)\left[\left(2 / \alpha^0\right) / \left(1 / \alpha^+ + 1 / \alpha^-\right)\right] \tag{47}$$

where

$$\alpha^0 = n\int_0^\infty \left\{\partial^2\varphi^{+-} / \partial r^2 + \left(2 / r\right)\left(\partial\varphi^{+-} / \partial r\right)\right\} g_{+-}(r) 4\pi r^2 dr \tag{48}$$

$$\alpha^+ = \left(n / 2\right)\int_0^\infty [\{\partial^2\varphi^{++} / \partial r^2 + 2 / r\left(\partial\varphi^{++} / \partial r\right)\} g_{++}(r) + \\ + 2\{\partial^2\varphi^{+-} / \partial r^2 + 2 / r\left(\partial\varphi^{+-} / \partial r\right)\} g_{+-}(r)] 4\pi r^2 dr \tag{49}$$

$$\alpha^- = \left(n / 2\right)\int_0^\infty [\{\partial^2\varphi^{--} / \partial r^2 + 2 / r\left(\partial\varphi^{--} / \partial r\right)\} g_{--}(r) + \\ + 2\{\partial^2\varphi^{+-} / \partial r^2 + 2 / r\left(\partial\varphi^{+-} / \partial r\right)\} g_{+-}(r)] 4\pi r^2 dr \tag{50}$$

and

$$\Delta_{BR} = \left(4\pi n / 3k_B T\right)\int_d^\infty \left(\partial\varphi^{+-}(r) / \partial r\right) g_{+-}(r) r^3 dr \tag{51}$$

where $\varphi^{ij}(r)$ is an effective inter-ionic potential between ions i and j. $g_{ij}(r)$ is the partial pair distribution function between ions i and j as defined in the previous section. In this equation, we can approximate that d is equal to the hard-core contact distance between cation and anion, if both ionic sizes are rigid. However, this assumption may not be always valid for the heavier atoms. Here, we will use the first maximum position of $g_{+-}(r)$ as the distance of ionic contact. The quantity Δ_{BR} is essentially caused by an asymmetric distribution of the surrounded ions around the centered ion under an applied external field; it was obtained by Berne and Rice (Berne & Rice, 1964), and recently certified by the present authors in a different way (Koishi & Tamaki, 2005). Since it was found that values of α^0, α^+ and α^- are numerically close to one another, we can take $\Delta \sim \Delta_{BR}$ as the deviation from Nernst-Einstein relation in a molten salt.

The effective potential $\varphi^{+-}(r)$ shown in Eq.(48) is equal to the potential of mean force acting on the ion at the origin from other ion of opposite sign located at the distance r, and therefore it is possible to use the potential of mean force $U^{+-}(r)$, instead of $\varphi^{+-}(r)$. Therefore, equation Eq.(51) is converted to,

$$\Delta_{BR} = \left(4\pi n / 3k_B T\right)\int_d^\infty \left(\partial U^{+-}(r) / \partial r\right) g_{+-}(r) r^3 dr = -\left(4\pi n / 3\right)\int_d^\infty \left(\partial g_{+-}(r) / \partial r\right) r^3 dr \tag{52}$$

We can basically calculate the deviation from Nernst-Einstein relation, by using Eq.(52), if $g_{+-}(r)$ is experimentally obtained. However, because of the presence of the r^3 term in the integrand, convergence at large r is slow and full information on the approach of $g_{+-}(r)$ to unity is necessary. At the present stage, $g_{+-}(r)$'s in molten salts being satisfactory this requirement seem to be rare.

3. Application of the theory to the real systems

In this section, the new theory of the dielectric screening is applied to the real systems to test the validity of the theory utilizing the structure factors obtained by simulation or experiment. The theory is applied to molten alkali-halides (Koishi et al., 2007), and noble metal halides (Matsunaga et al, 2007, 2008, 2011). We summarize the results in the following subsections. Application to molten AuCs is also mentioned.

3.1 Inverse dielectric function in molten NaCl obtained by computer simulation

It is not necessary to apply the dielectric function for the computer simulation, because the simulation procedure itself involves automatically the screening behaviors and only the utilization of appropriate bare inter-ionic potentials is required, although the ion's charges are not always equal to their valence ones. In fact, the effective charge z* used in computer simulation is sometimes smaller than the ion's valence number because of a partly covalent character of the constituents. In the cases of MD or Monte-Carlo simulations, the effective charge in molten CuI is taken to be 0.6 (Waseda et al., 2000). In this section, we derive the charge-charge correlation function Szz(q) and the inverse dielectric function $1/\varepsilon(q)$ of molten NaCl by using MD simulation. The well-known Tosi-Fumi potentials are used as the bare inter-ionic potentials. The simulated $g_{++}(r)$, $g_{--}(r)$ and $g_{+-}(r)$ in the range of r < 8Å agreed with the experimental results (Edwards et al., 1975) and indicate a good isotropic configuration suggesting $\delta = 1$ and these quantities were inserted into Eq.(4). The obtained Szz(q) of molten NaCl is shown in Fig.1, which agreed with that shown in the literature (Hansen & McDomald,1986). Putting this Szz(q) into (19-a), we have $1/\varepsilon(q)$ in molten NaCl as shown in Fig.1. Using the obtained $1/\varepsilon(q)$ and taking α=0.5 as a trial screening factor for the repulsive potential and (33-a), the estimated screened potential between cation and anion is shown in Fig.2. So far the obtained screened potential is, more or less, close to the mean force $U^{+-}(r)$. A difference between $\varphi^{+-}{}_{sc}(r)$ and $U^{+-}(r)$, which are shown in Fig.2, may be caused by several reasons. One of them is that the inverse dielectric function is only applicable for a gradual slope of attractive potential and the screening for the repulsive part is restricted to a qualitative way as multiplying the parameter α. This treatment may diminish more or less, the exactness of the result. The other reason is that we have used Tosi-Fumi potential for MD simulation in order to obtain $g_{+-}(r)$. Even though the obtained $g_{+-}(r)$ by this simulation is close to the experimental one in the range r < 8Å, we are not sure of the possibility of the agreement in the range of the distance beyond 8Å, because the decaying tendency of $g_{+-}(r)$ obtained by simulation is slow, indicating a remarkable oscillation up to r = 15Å. Usually it is hard to obtain any visible oscilation in the experimental $g_{+-}(r)$ beyond the distance of r ~ 10Å. It is known that a Monte-Carlo simulation using the deformed dipole model (Gartrell-mills & McGreevy, 1989), which makes it possible to have a more rapid decaying for $g_{+-}(r)$, gives better agreement for the experimental results of molten CsCl (Locke et al., 1985). These

facts suggest that the second and third peaks of $U^{+-}(r)$ obtained from simulated $g_{+-}(r)$ should be diminished to some extent in the range of r > 10 Å. At the present stage, the obtained $\varphi^{+-}_{sc}(r)$ is inevitably somewhat numerically different from $U^{+-}(r)$. By inserting the calculated $\varphi^{+-}_{sc}(r)$ instead of $U^{+-}(r)$, however, the obtained $g_{+-}(r)$ is semi-quantitatively close to the simulated one, as shown in Fig.2.
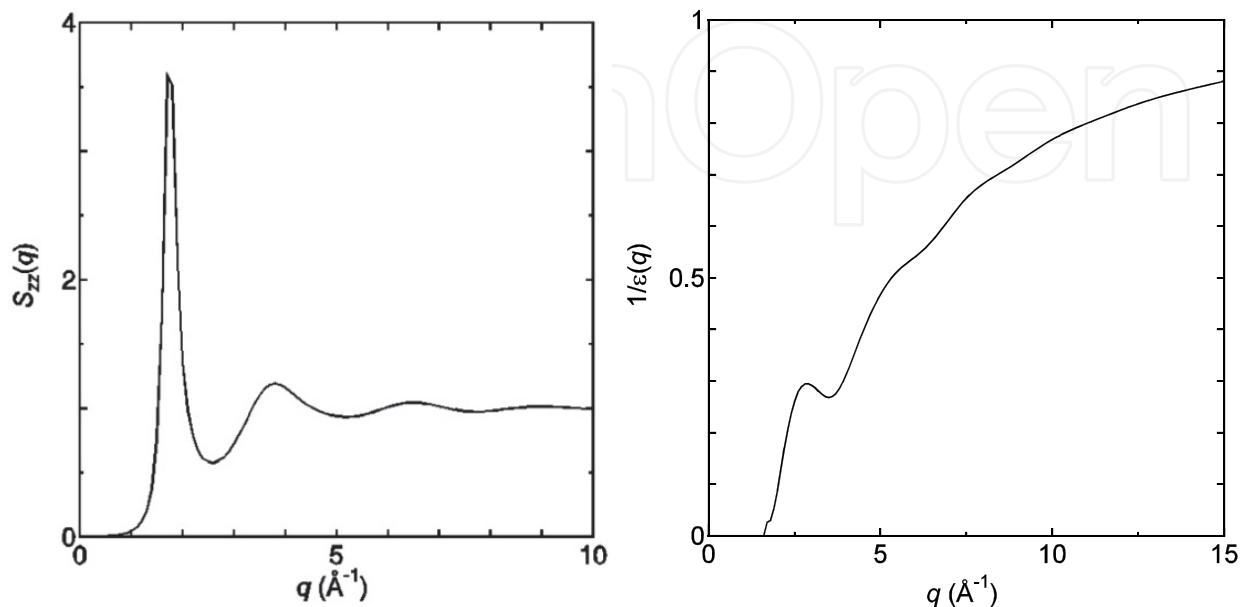

Fig. 1. $S_{ZZ}(q)$ of molten NaCl obtained by MD (left), $1/\varepsilon(q)$ of molten NaCl (right),
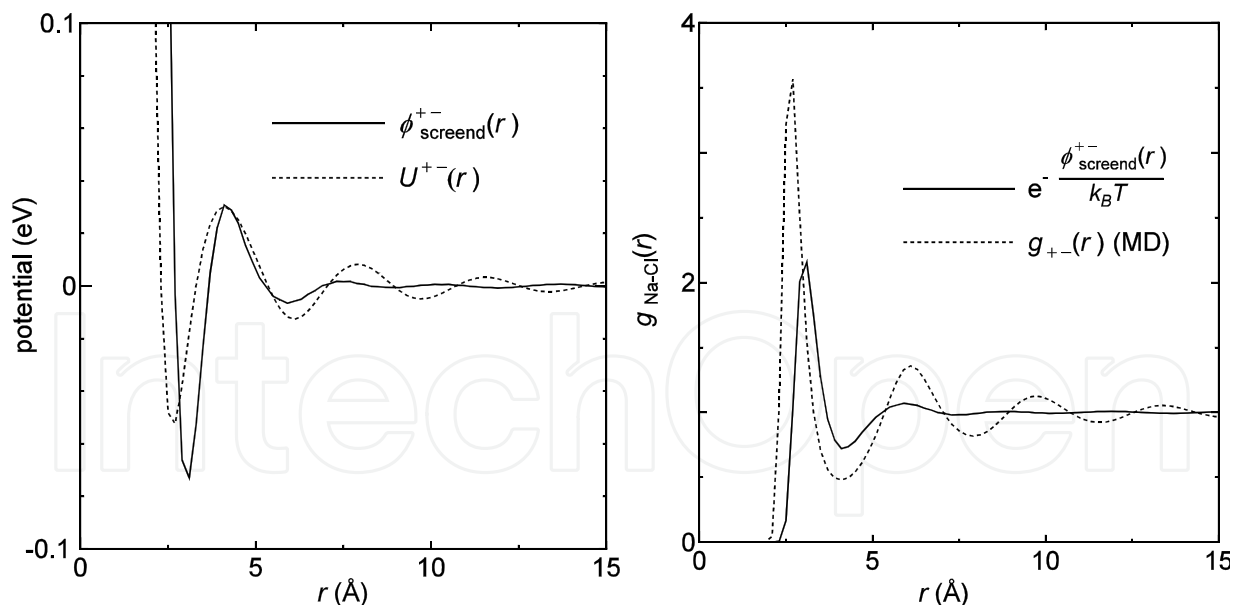
Fig. 2. $\varphi^{+-}_{sc}(r)$ and $U^{+-}(r)$ (left), $g_{+-}(r)$ and $\exp(-\varphi^{+-}_{sc}(r)/k_BT)$ (right) of molten NaCl.

3.2 Inverse dielectric function for molten RbBr obtained from experimental $S_{\nu\mu}(q)$

In this section we will show $1/\varepsilon(q)$ of molten RbBr, using the experimental partial structure factors. The experimental data for $S_{\nu\mu}(q)$ are adopted from the articles observed by Saito et al.(1999). In Fig.3, the experimentally obtained $S_{zz}(q)$ and the corresponding

$1/\varepsilon(q)$ are shown. As seen in these figures, the larger $S_{zz}(q)$ rather than unity yields a relatively small $1/\varepsilon(q)$. This fact is physically plausible, because a large charge fluctuation at the position of r around a centered ion located at the origin indicates a larger distribution of ions of opposite sign at r, which naturally causes a large screening in comparison with that of an averaged distribution of ions.

Using available repulsive potential for molten RbBr (Saito et al., 1999), we have calculated the screened potential by putting the appropriate $1/\varepsilon(q)$ into equation (33-a). The results are shown in Fig.4 under the condition of $\alpha=1$. As seen in Fig.4, the screened inter-ionic potential between Rb^+ and Br^- ions, $\varphi^{+-}_{sc}(r)$ has deeper minimum in comparison with the potential of mean force, $U^{+-}(r)$, contrasting with the tendency of molten NaCl starting from the partial structure factors obtained by MD simulation. The most likely reason for this discrepancy seems to be an experimental uncertainty for partial structure factors in their small-q regions. This uncertainty gives, in due course, a numerical error in the inverse dielectric function $1/\varepsilon(q)$ in the very small-q region, even though its magnitude is relatively small. On Fourier transformation, such a small uncertainty gives a remarkably large change in the screened inter-ionic potential. In fact, an artificial modification for the curve of $1/\varepsilon(q)$ in only the small-q region makes it possible to obtain a result similar to $U^{+-}(r)$.
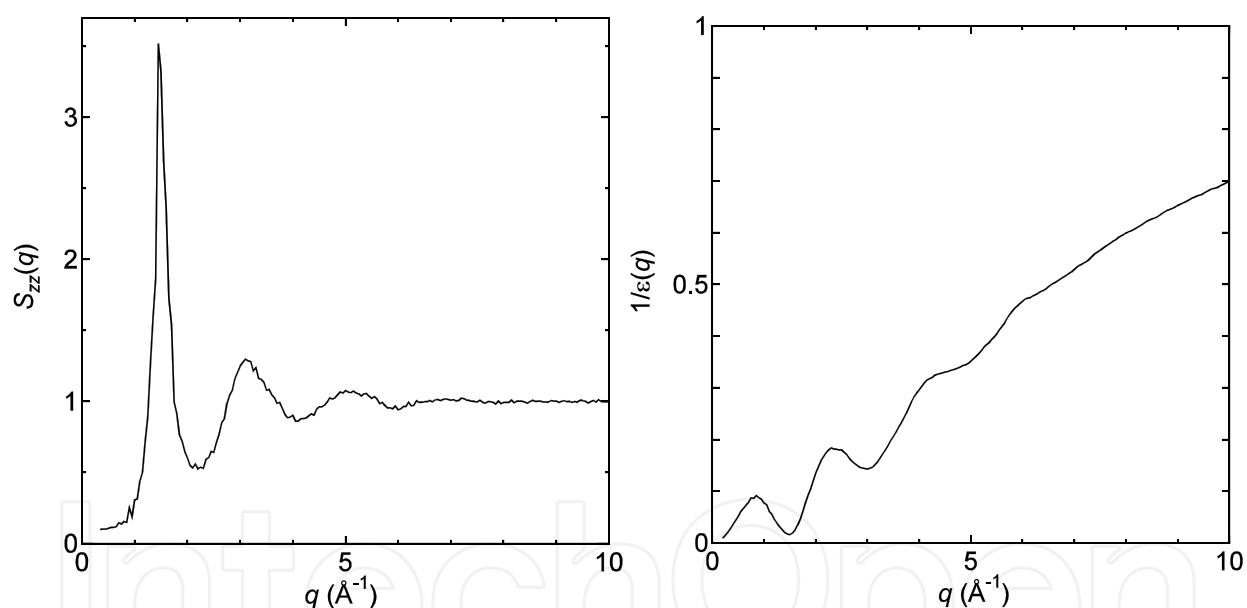

Fig. 3. Experimental Szz(q) (left), and $1/\varepsilon(q)$ (right) of molten RbBr.

3.3 Dielectric screening properties in molten noble metal halide and their mixtures

In this subsection, we focuse on molten noble-metal halides, AgBr and CuBr (Matsunaga et al., 2008), and mixture AgI-AgBr system (Matsunaga et al., 2007). It is well known that the noble metal halides are the typical example of the superionic conductors, which is a group of substances that exhibits high values of ionic conductivity, while they are still in solid phase. The mechanism of high ionic conductivity in the superionic conductors has been widely investigated because of their novel physical behaviour and technological importance, *e.g.* solid state batteries, fuel cells, optical devices (see for example, Chandra, 1981). CuBr shows superionic conduction in its alpha phase, where copper ions statistically

distribute around the bromine bcc cubic, and copper ions can move one site to another. However, AgBr has a rock salt structure in its solid state and does not exhibit superionic conduction until its melting temperature, though AgBr is also one of the noble metal halides. We have investigated the structural and transport properties of noble metal halide mixtures by molecular dynamics simulations (Matsunaga, 2003; Matsunaga & Madden, 2004; Matsunaga, 2005). In this subsection, we apply the new theory to molten AgBr, CuBr , and AgI-AgBr to examine the dielectric screening effect, because the screened potentials are the fundamental subject for the transport properties.
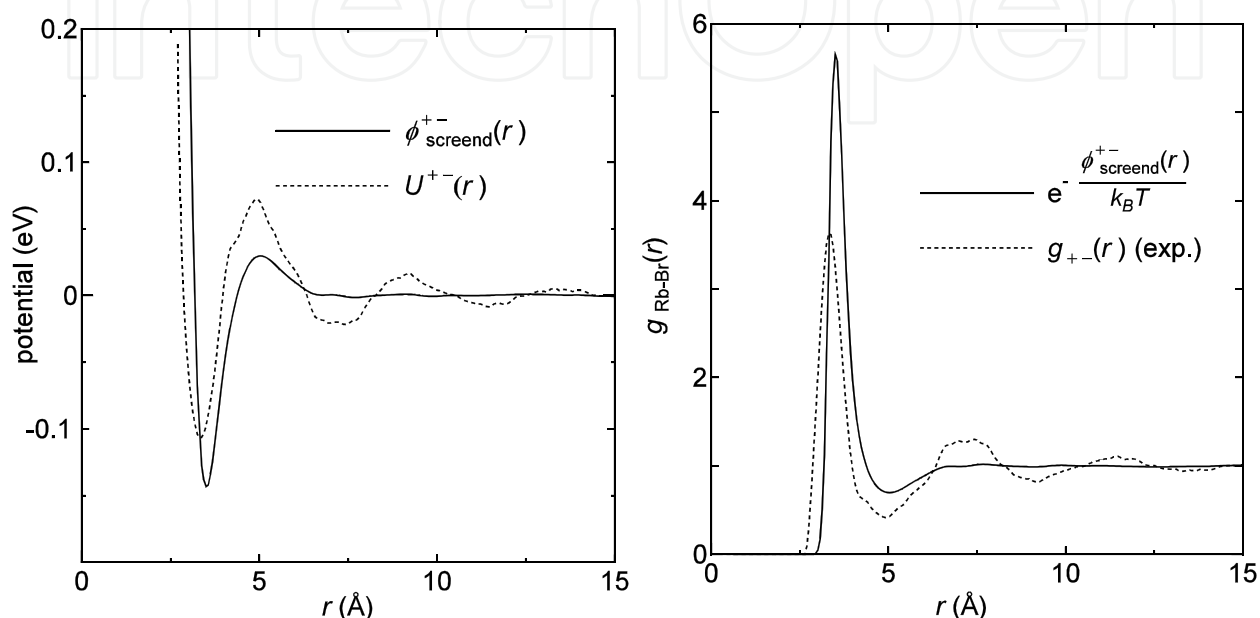
Fig. 4. $\varphi^{+-}_{sc}(r)$ and $U^{+-}(r)$ (left), $g_{+-}(r)$ and $\exp(-\varphi^{+-}_{sc}(r)/k_BT)$ (right) of molten RbBr.
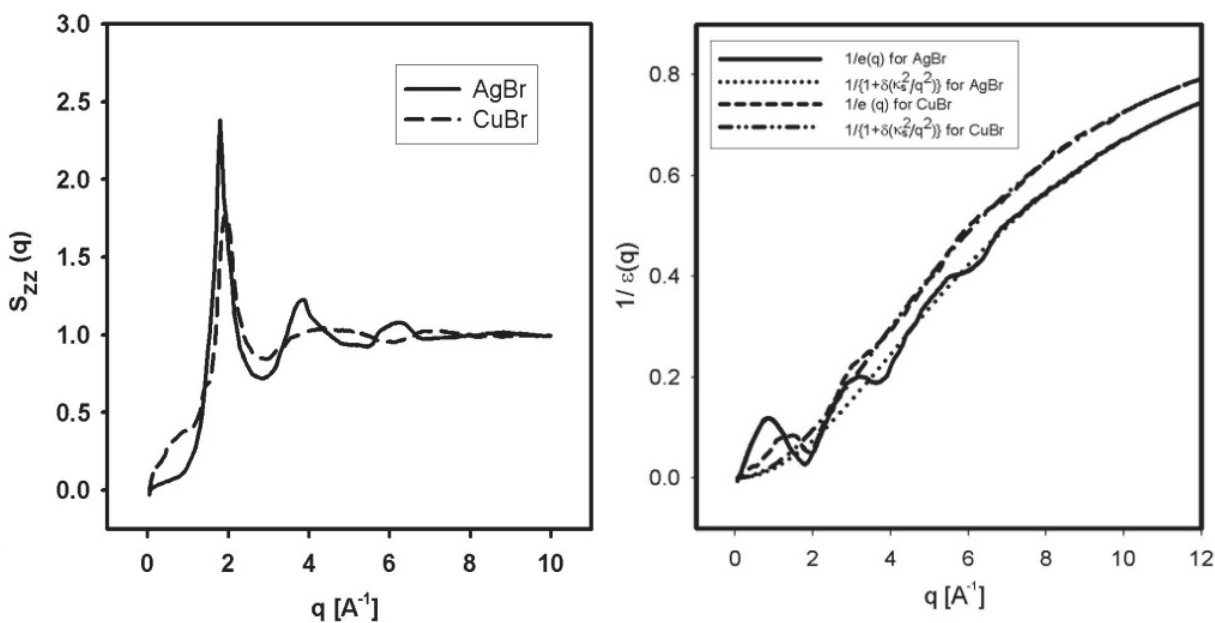

Fig. 5. $S_{ZZ}(q)$ (left), and $1/\varepsilon(q)$ with $1/(1+\delta(\kappa_s^2/q^2))$ for AgBr and CuBr (right).

As mentioned before, Eq.(19-a) or Eq.(20) is useful to derive $1/\varepsilon(q)$ from the experimental partial structure factors. Eq.(3) is applicable to deriving $1/\varepsilon(q)$ from $g_{+-}(r)$ by computer simulation. For examples of $1/\varepsilon(q)$ for binary ionic melts, we will show the results of $1/\varepsilon(q)$ using experimental $S_{ZZ}(q)$ for AgBr and CuBr (Saito et al., 1997; Saito et.al., 1999). As mentioned previously, $S_{ZZ}(q)$ is related to structure factors and pair distribution functions by Eq.(2). In this case, the summation in Eq.(2) is taken for ion species Ag or Cu and Br. The obtained $S_{ZZ}(q)$ for molten AgBr at 753K and CuBr at 810K are shown in Fig.5. We can see the significant first peaks in $S_{ZZ}(q)$ at about 1.8Å^{-1} and 2.0 Å^{-1} for molten AgBr and CuBr, respectively. These peaks correspond to the oscillations of partial structure factors (Saito et al., 1997; Saito et.al., 1999). By substituting these $S_{ZZ}(q)$ into Eq.(20), we can obtain the inverse dielectric function $1/\varepsilon(q)$. The calculated results are shown in Fig.5 with the calculated curve by Eq.(21) for comparison. It is clearly recognized that $1/\varepsilon(q)$ satisfies the condition $0 \leq 1/\varepsilon(q) \leq 1$. We can find the oscillatory features and the significant minimum at around 1.8 Å^{-1} and 2.0 Å^{-1} for AgBr and CuBr, respectively. These features are yielded by the form of $S_{ZZ}(q)$'s which have large maximum and oscillation. These results should be attributed to the effect that an ion in molten salts is estimated to be surrounded by ions of opposite sign, which yields the large charge fluctuation and screening effect.
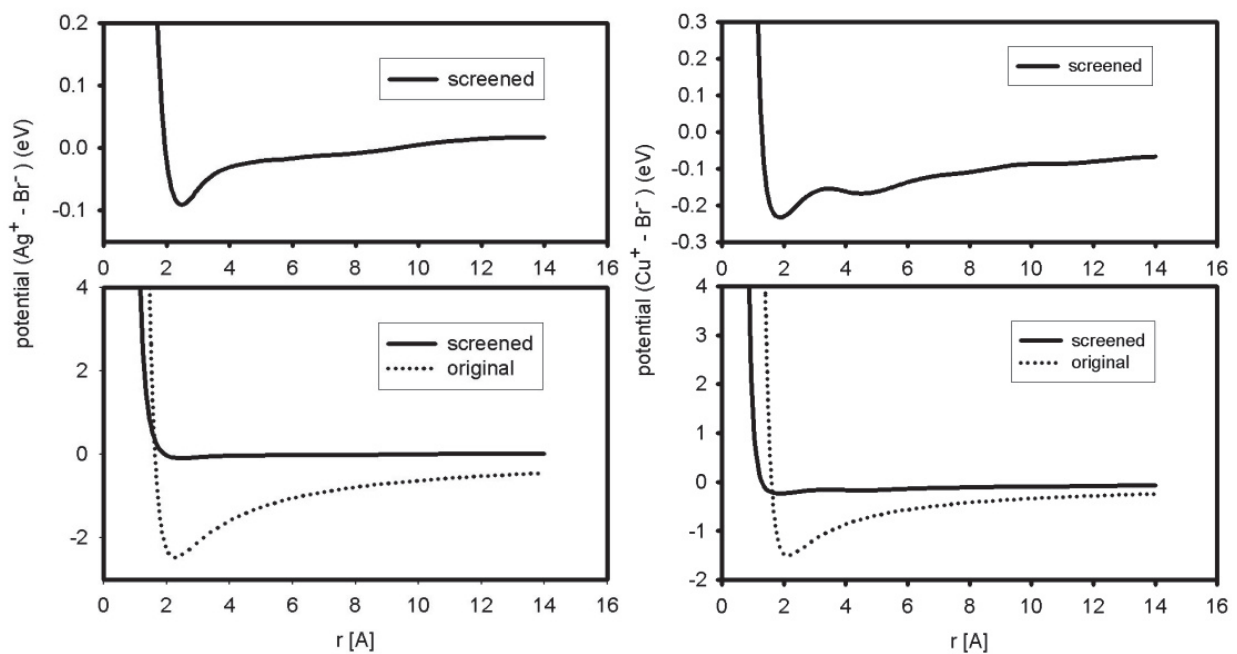

Fig. 6. Screened potential for Ag-Br (left) and Cu-Br (right) with original one (bottom). Screened potentials are also shown with different scale to show their oscillatory feature (top).

From above consideration, it seems interesting to obtain the screened potential between anion and cation, Ag^+ or Cu^+ and Br^- in molten AgBr and CuBr. Besides, the experimental pair distribution functions between cation and anion, *i.e.* $g_{BrAg}(r)$ and $g_{BrCu}(r)$ are obviously different (Saito et al., 1997; Saito et.al., 1999). We adopt the potential by Rahman, Vashishta and Parrinello (RVP) (Parrinello et al., 1983), as bare inter-ionic interaction. The RVP type potential sets for i and j ions are written as,

$$V_{ij}(r) = H_{ij} / r^{n_{ij}} + z_i z_j e^2 / r - P_{ij} / r^4 \tag{53}$$

where the third term is charge-dipole interactions. The adopted parameters are taken from literature (Tasseven et al., 1997; Stafford et al., 1990). The screened potentials of molten AgBr and CuBr are obtained by the procedure described in the previous sections. The results are shown in Fig.6. In the calculation, we adopt the value of δ as 0.50 and 0.40, and the value of α as 0.1 and 0.05 for AgBr and CuBr, respectively. The reduction of the depth of potential by screening effect is obviously recognized in Fig.6. The characteristic oscillations are found in the screened potentials especially in molten CuBr, which may be caused by the charge fluctuation in the distribution of ions.
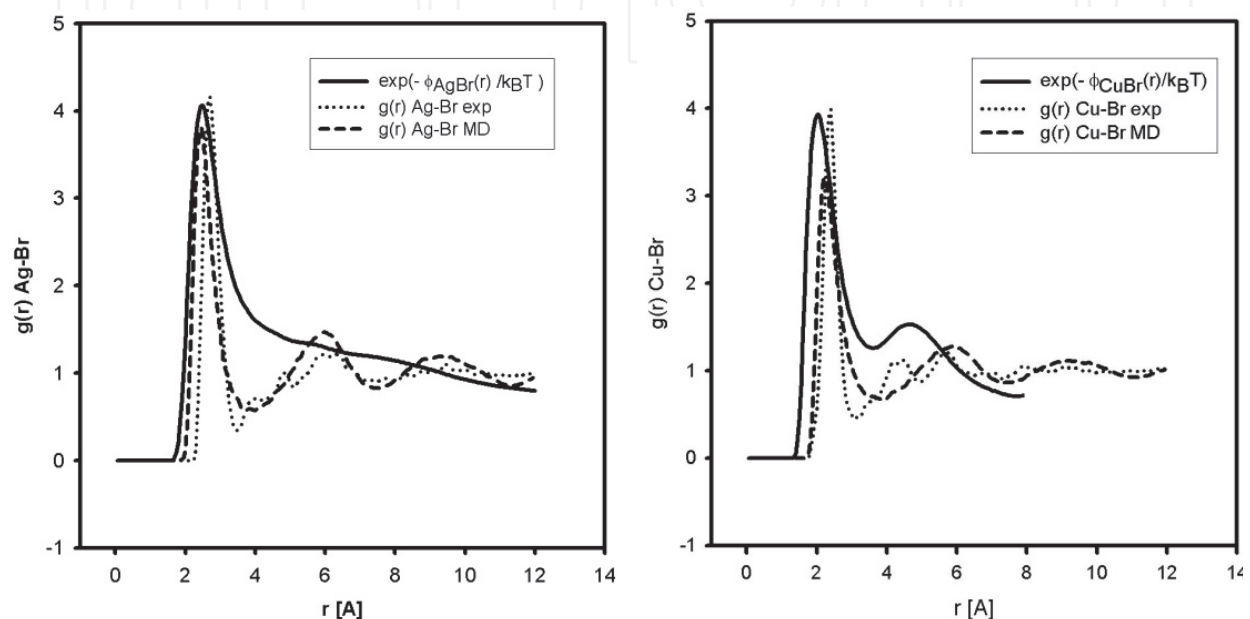

Fig. 7. $_{ij}$(r) for AgBr (left) and CuBr (right) calculated using screened potential with that by experiment and by MD.

To confirm the results of screened potentials between cations and anions, we calculate the pair distribution function $g_{+-}(r)$ by the potential of mean force $U^{+-}(r)$, which is defined by Eq.(37-a), where we can take the screened potential $\varphi^{+-}_{sc}(r)$ as $U^{+-}(r)$, because Eq.(37-a) is originally suggested by weak interacting materials. In the previous section, we have proved that $\varphi^{+-}_{sc}(r)$ and $U^{+-}(r)$ are mathematically equivalent, being our argument based on the Ornstein-Zernike equation (Koishi et al., 2007). $g_{+-}(r)$ are obtained by inserting the calculated $\varphi^{+-}_{sc}(r)$ instead of $U^{+-}(r)$ into Eq.(37-a). They are shown in Fig.7, together with $g_{+-}(r)$'s obtained by experiment and molecular dynamics (MD) simulation. The first peaks of $g_{+-}(r)$ almost agree well, though the oscillations in larger r region are not satisfactory reproduced. This fact may suggest that the screening effect is considerable especially in the small r region, *i.e.* about the distance to the first nearest neighbors. In other words, the first nearest neighbor ions have the main contribution to the screening effects in molten salts.

Next, we apply the theory to molten AgI-AgBr as an example of a pseudo-binary system, in which ions are thought to be in considerable order. It is well known that silver iodide is one of the superionic conductors in its alpha phase, i.e. α-AgI, in which silver ions statistically distribute around the iodine bcc cubic. On the other hand, AgBr has a rock salt structure in its solid state and dose not exhibit high conduction. We have investigated the

effect of dissolution of AgBr into AgI on the structural and transport properties in superionic and molten phases by molecular dynamics simulations (Matsunaga, 2005).

Accordingly it is interesting to discuss the dielectric screening effects in this system. We wish to show the result for $1/\varepsilon(q)$ by using $S_{ZZ}(q)$ obtained by simulation. Though the consideration to this point is for the equi-charged binary salts, the theory is easily extendable to the equi-charged pseudo binary molten salts, e.g. AgI-AgBr, and Eq.(19-a) is also applicable to them. As mentioned in the previous section, $S_{ZZ}(q)$ is related to structure factors and pair distribution functions as Eq.(2), $S_{ZZ}(q) = \Sigma_\nu \Sigma_\mu z_\nu z_\mu S_{\nu\mu}(q)$, where summation is taken for species Ag, Br and I. We derive $1/\varepsilon(q)$ from the structure factors obtained by molecular dynamics simulation. The procedure of the simulation is essentially same as the previous work (Matsunaga, 2005). The RVP type pair potential sets are used, which parameters are listed in the same reference. The I-Br interaction is estimated by the appropriate combination rule. The MD calculations are performed for $Ag(Br_xI_{1-x})$ (x=0.20) at 903K.

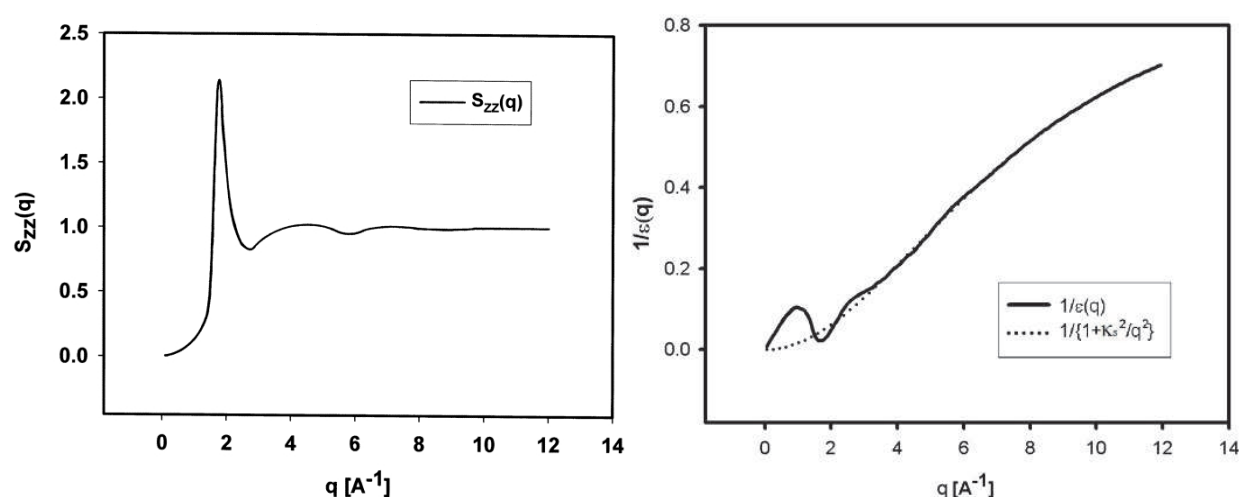Fig. 8. $S_{ZZ}(q)$ (left), $1/\varepsilon(q)$ and $1/\{1+\kappa_s^2/q^2\}$ (right) for $Ag(Br_xI_{1-x})$ (x=0.20) at 903K.
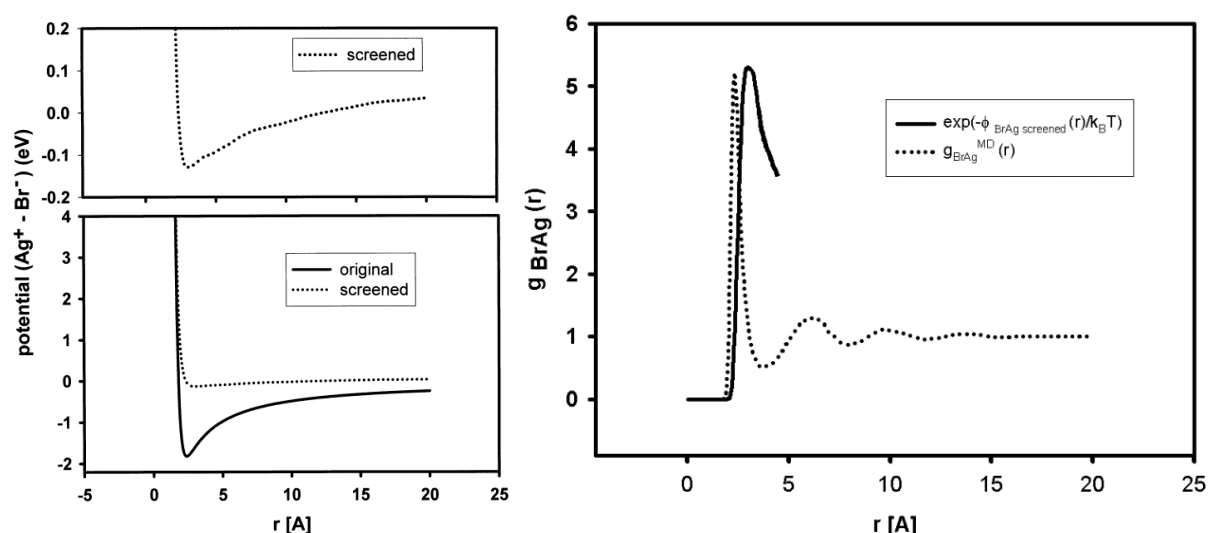

Fig. 9. The screened potential between Ag and Br with original one (left bottom). The screened potential is also shown in different scale (left top). $g_{ij}(r)$ calculated using screened potential with that obtained by MD (right).

The obtained $S_{ZZ}(q)$ at 903K is shown in Fig.8. We can see a significant peak in $S_{ZZ}(q)$ at about 1.7Å^{-1} and a plateau around 4.0Å^{-1} corresponding to the oscillations of partial structure factors (Matsunaga, 2005). We have the inverse dielectric function $1/\varepsilon(q)$ by putting obtained $S_{ZZ}(q)$ into Eq.(19-a), which is shown in Fg.8 with that calculated by Eq.(21) for $\delta=1$ for comparison. It is clearly recognized that $1/\varepsilon(q)$ satisfies the condition Eq.(27). We can see the significant minimum at around 1.7Å^{-1} corresponding the large maximum of $S_{ZZ}(q)$, which shows the large charge fluctuation. This fact may be attributed to the effect that an ion at the origin is supposed to be surrounded by ions of opposite sign at position r, which may yield the large charge fluctuation and screening effect.

The discrepancy in the larger r region between $g_{+-}(r)$'s are attributed to the difference between $\varphi^{+-}{}_{sc}(r)$ and $U^{+-}(r)$, which may be caused by several reasons, in addition to a margin of calculation error in Fourier transformation. One reason is that only the Coulomb attractive potential is used to derive $\varphi^{+-}{}_{sc}(r)$ instead the attractive part of RVP type potential $-P_{ij}/r^4$ which is used for simulation. Another possible reason is that the non-symmetric structure in solid phase remains in molten phase, which may obstruct the screening effect in molten phase. In spite of above facts, however, it may be recognized that the calculated result for $\varphi^{+-}{}_{sc}(r)$ so as to carry on the above treatment is physically significant, and the obtained results are obviously affected by screening effect.

3.4 Cation-cation interaction in noble metal halide mixtures

In the superionic phase of noble metal halides, the distributions of cations have been studied in detail. These studies have been executed mainly in the systems with one kind of cation, *i.e.* Cu^+ or Ag^+, that is supposed to be distributed mainly around the tetrahedral 12(d) site of halogen bcc lattice. However, according to the recent experimental study by NMR and X-ray diffraction, cations Cu^+ and Ag^+ are distributed mainly around the octahedral 6(b) site in the superionic phase of $(Ag_xCu_{1-x})I$, which is contradictory to the generally accepted view (Endo et al., 1999). Besides the interest on the basis of physical chemistry, there would be an advantage of practical application, because the pseudo-binary superionic conductor may lower the transition temperature to the superionic phase. These facts prompt us to investigate the superionic phase of noble metal halide mixture with two kinds of mobile cations. In the previous study (Matsunaga, 2009), we have carried out the molecular dynamics (MD) simulation to examine the structural properties of $(Ag_xCu_{1-x})Br$ for $x < 0.5$ in its superionic phase as an example of the superionic conductor with two kinds of cations, Cu^+ and Ag^+. The MD results were quite noteworthy; the different distributions between Ag^+ and Cu^+ ions in superionic phase were detected. For $x_{Ag} = 0.10$, Cu ions are mainly distributed around the tetrahedral 12(d) site. On the other hand, the significant distribution of Ag ions around the octahedral 6(b) site can be seen. For $x_{Ag} = 0.40$, however, Cu ions are mainly distributed around the octahedral 6(b) site. Ag ions are also distributed around the octahedral 6(b) site, moreover their distribution is more enhanced than those in $x_{Ag} = 0.10$ (Matsunaga, 2009a). These results suggest that there is a concentration dependence in cation distribution for $(Ag_xCu_{1-x})Br$, which may affect the dynamical and thermodynamic properties of this system.

In this subchapter, considering the circumstances mentioned above, as a continuous work (Matsunaga, 2011), we investigate the dynamical and thermodynamic properties of the superionic and molten phases of $(Ag_xCu_{1-x})Br$ for $x < 0.5$ by MD. The essential procedure of MD simulations is same as our previous works (Matsunaga, 2009a, 2009b; Matsunaga &

Tamaki, 2008a, 2008b). *RVP* type pair potentials are used. The used potential parameters are taken from literature (Stafford et al.,1990; Tasseven et al., 1997) The interactions between cations are obtained using the adequate combination rule. The used potential parameter sets are listed in the Table 1 in the previous paper (Matsunaga, 2009a).

The concentration-concentration (C-C) structure factor is quite effective to clarify the structural features of the molten binary system, which have been obtained by the experiments (Bhatia & Thornton, 1970; Matsunaga et al., 1983). The C-C structure factor has also been extended to the multi component systems (Bhatia & Ratti,1977). In this subsection, the C-C structure factors will be evaluated to examine how the structural features in the superionic phase of the system $(Ag_{1-x}Cu_{0x})Br$ will be observed in the molten phase. The procedure to obtain the multi component C-C structure factor is briefly summarized as follows. The partial structure factor defined by Faber and Ziman is expressed as,

$$a_{ij}(q) = 1 + \frac{N}{V}\int\{g_{ij}(q) - 1\}e^{iq\cdot r}d^3r \qquad (54)$$

where $g_{ij}(r)$ is the pair distribution function, and i and j stand for the species of ions. The multi component C-C structure factor, $Sc_ic_j(q)$, is defined as,

$$S_{c_ic_j(q)} = \frac{1}{2}N\langle c_i^*(\boldsymbol{q})c_j(\boldsymbol{q}) + c_i(\boldsymbol{q})c_j^*(\boldsymbol{q})\rangle \qquad (55)$$

$Sc_ic_j(q)$ is related to the Faber-Ziman type structure factor $a_{ij}(q)$ as,

$$Sc_ic_j(q) = c_ic_j\left(a_{ij}(q) - \sum_{\xi=1}^{\nu}c_\xi\left(a_{i\xi}(q) + a_{j\xi}(q)\right) + \sum\sum_{\xi\zeta=1}^{\nu}c_\xi c_\zeta a_{\xi\zeta}(q)\right) + c_i\delta_{i,j} - c_ic_j \qquad (56)$$

where ξ and ζ also stand for the species of ions. ν is the number of the species. In the case of the '*ideal*' mixture, $Sc_ic_j(q)$'s for the long wave length limit, $q \to 0$, are expressed as,

$$S_{c_ic_i}^{id}(0) = c_i(1 - c_i), \qquad S_{c_ic_j}^{id}(0) = -c_ic_j \qquad i \neq j \qquad (57)$$

The obtained normalized $Sc_ic_j(q)$'s divided by $|S^{id}c_ic_j(0)|$ in the molten phase 76K above the liquidus are shown in Fig.10. The difference between $Sc_{Ag}c_{Ag}(q)$ and $Sc_{Cu}c_{Cu}(q)$ can be seen in both figures. In Fig.10 for $(Ag_{0.1}Cu_{0.9})Br$, the profile $Sc_{Ag}c_{Ag}(q)\simeq1$ shows the weak interaction between Ag ions, thought the interaction between Cu ions and between Cu and Ag ions seems to be significant in $Sc_{Cu}c_{Cu}(q)$ and $Sc_{Ag}c_{Cu}(q)$. The peaks in $Sc_{Ag}c_{Ag}(q)$ can be seen at about 3.6 and 1.8Å^{-1}; in $Sc_{Cu}c_{Cu}(q)$ at 4.9 and 1.8 Å^{-1}; in $Sc_{Ag}c_{Cu}(q)$ at 3.6 and 1.8 Å^{-1} corresponding to the first and the second nearest neighbors, respectively. In Fig.10 for $(Ag_{0.4}Cu_{0.6})Br$, the interaction between Ag ions seems to be somewhat enhanced in $Sc_{Ag}c_{Ag}(q)$, though the interaction between Cu ions is decreased. The interaction between Ag and Cu ions is still significant in $Sc_{Ag}c_{Cu}(q)$. The peaks in $Sc_{Ag}c_{Ag}(q)$ can be seen at about 3.7 and 1.8 Å^{-1}; in $Sc_{Cu}c_{Cu}(q)$ at 5.0 and 1.9 Å^{-1}; in $Sc_{Ag}c_{Cu}(q)$ at 3.8 and 1.9 Å^{-1} corresponding to the first and the second nearest neighbors, respectively.

The expression of $Sc_ic_j(q)$ for the long wave length limit, $q \to 0$, is related to the correlation between the fluctuations Δc_i and Δc_j as follows:

$$Sc_ic_j(0) = N < \Delta c_i\Delta c_j > \qquad (58)$$

which has a physical meaning of an order parameter in the molten state (Bhatia & Ratti, 1977; Bhatia & Thornton, 1970). $Sc_ic_j(0)$ is related to the thermodynamic quantities. In a ternary system, e.g. $Sc_1c_2(0)$ is expressed as

$$S_{c_1c_2}(0) = -c_1c_2 \left\{ 1 + \frac{c_3(\omega_{12}-\omega_{13}-\omega_{23})}{k_BT} \right\} / D \tag{59}$$

where D is the function of ω_{ij}. ω_{ij}'s are the pairwise interchange energies which are related to the excess free energy G^E as follows:

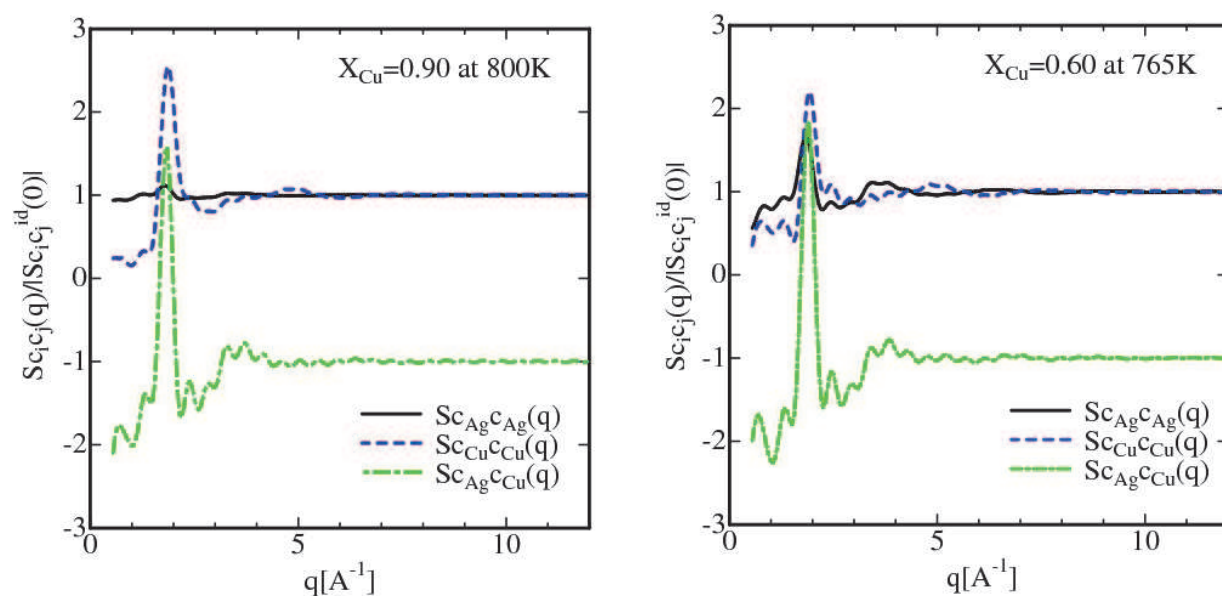$$G^E = N \sum \sum_{\alpha < \beta} c_\alpha c_\beta \omega_{\alpha\beta} \tag{60}$$

Fig. 10. $S_{c_ic_j}(q)/|S_{c_ic_j}^{id}(0)|$ for $(Ag_{1-x}Cu_x)Br$, $x_{Cu}=0.9$ at 800K (left), $x_{Cu}=0.60$ at 765K (right).

Though G^E for molten $(Ag_xCu_{1-x})Br$ is not available as far as we know, the expected values from the MD result in the superionic phase are $|Sc_{Ag}c_{Cu}(0)| > |S^{id}c_{Ag}c_{Cu}(0)|$ for $x_{Cu} = 0.90$, $|Sc_{Ag}c_{Cu}(0)| \leq |S^{id}c_{Ag}c_{Cu}(0)|$ for $x_{Cu} = 0.60$. In other words, the phase separation tendency of Ag and Cu ions for $x_{Cu} = 0.90$, and the ordering tendency for $x_{Cu} = 0.60$. This fact suggests that there is the concentration dependence of the interaction between ions, ω_{ij}, in molten phase.

As stated so far, there is a concentration dependence in the dynamical and thermodynamic properties as well as the structural feature in the superionic and molten phases for $(Ag_xCu_{1-x})Br$, which suggests the many body effects and the short range interaction in the molten ternary system.

4. Polarizable ion model and dielectric screening effect

To understand qualitatively and quantitatively the properties of molten salts such as the static and dynamical behaviour, theoretical and molecular dynamics simulation studies are indispensable. For this purpose, the main problem is how to define the appropriate pair-

potentials for the system of one's study. Needless to say, the properties of molten salts are, more or less, related with those of the solid phase. There are various ionic crystals; alkali-halides with rock salt structure which has ionic bond; zinc-blend (ZnS) type in which covalent and ionic bond coexist; superionic conductor of which a typical representative is AgI; etc. The constant efforts have been made for about 80 years to study the inter ionic potentials for these ionic crystals of various ionisation (Matsunaga & Tamaki, 2011). In this study, we will show how the theory of screened potentials is modified in connection with the recent development. The new theory will be applied to copper iodide for example. The numerical results will be discussed in comparison with those of experiment and molecular dynamics (MD) simulation.

4.1 Polarizable ion model

In recent years, studies have been developed on the viewpoint of the charge distribution change in a certain ion caused by approaching of surrounding ions. In 1996, Wilson et al. succeeded to perform MD to reproduce the experimental results of molten AgCl structure using new potentials introducing ion polarization. In 2006, Bitrián and Trullàs proposed the similar polarizable ion model to perform MD simulation in molten AgBr. In this case, Vashishta-Rahman (VR) type potential is adopted as the rigid ion model potential (Vashishta and Rahman, 1978), which is familiar in the study of super ionic conductor, expressed as follows,

$$\varphi_{ij}(r) = \frac{z_i z_j e^2}{r} + \frac{H}{r^n} - \frac{C_{ij}}{r^6} - \frac{P_{ij}}{r^4} \equiv \varphi_{ij}^0(r) - \frac{P_{ij}}{r^4} \tag{61}$$

where, n=7 power term is adopted for the repulsive potential in the second term on the right hand side. The dipole-quadrupole interaction term is neglected, because it is smaller than the last two terms in Eq.(61). The feature of the polarizable ion model is that the charge-dipole interaction or the last term in Eq.(61), P_{ij}/r^4, is expressed as a function of r, which may be the origin of its name '*polarizable*'. In the polarizable ion model, introducing the dumping function $f_{ab}(r)$ which varies from 0 to 1, the dipole of ion a by the surrounding ion b is expressed as follows,

$$p_a = \alpha_a \{1 - f_{ab}(r)\} \{(z_b e / r^2) + (2\alpha_b z_a e / r^5)\} / \{1 - (4\alpha_a \alpha_b / r^6)\} \tag{62}$$

which means $p_a(r)$ diverges at $r_c^6 = (4\alpha_a \alpha_b)$, where α_i is the polarizability of ion i. This singular point is called *the polarization catastrophe distance*. This divergence is ascribed to the fact that the iteration has been done disregarding that r_{ij} is required much longer than the distance between the positive and negative dipole charges. Therefore, strictly speaking, the equations of polarizable model are valid only in the case when the polarizability of the ion a or b is almost zero. In the molten state of Ag or Cu halide including super ionic conductor, e.g. AgI, AgBr, Ag$_2$Se, Ag$_2$Te, CuBr etc., the dipole moments of cations are considerably smaller than those of anions, hence $r_c^6 \sim 0$ (see, e.g. tables in Kittel,1996). Consequently, the condition $\alpha_+ \sim 0$ would be strictly applicable to the pair potentials $\varphi_{+-}(r)$ and $\varphi_{++}(r)$. From the considerations based on these facts, the polarizable ion model has been applied to AgBr and AgCl (Bitrián and Trullàs, 2006 ; Wilson et al., 1996).

4.2 Evaluation of polarizable ion model in the previous section

The theory that Bitrián and Trullàs (2006) have developed is effective to revise the rigid ion model to some extent. However, as we have pointed out in the previous section, such dispersion called *the polarization catastrophe* is ascribed to the fact that the iteration has been done disregarding that the inter ionic distance r_{ij} is required to be much longer than the distance between the positive and negative dipole charges. In fact, for example, the polarization catastrophe distance in molten NaCl estimated from the electron polarizabilities of Na and Cl ions is 0.93A. Of course the actual negative increasing of potential to the catastrophe would be relaxed to some extent, as the short range damping factor $f_{ab}(r)$ rapidly approaches to 1. In spite of these facts, it is quite doubtful whether that is the effective theoretical value when *r* approaches to the nearest ionic distance.

Because the $f_{ab}(r)$ is used as a parameter, the following *a prior* expression seems to be more preferable, as,

$$\varphi_{ab}(r) = \varphi_{ab}{}^0(r) - P_{ab} / r^4 = \varphi_{ab}{}^0(r) - (1/2)\{1 - f_{ab}(r)\}^2 (\alpha_a z_b{}^2 e^2 + \alpha_b z_a{}^2 e^2) / r^4 \qquad (63)$$

Though $f_{ab}(r)$ in Eq.(63) is different from those Wilson et al. (1996), or Bitrián and Trullàs (2006) have defined, the function which satisfies the following condition will be appropriate; when *r* approaches to 0, then $f_{ab}(r)$ approaches to 1; when *r* increases (about twice of the inter ionic distance), $f_{ab}(r)$ approaches to 0. In any case, by setting $f_{ab}(r)$ as Eq.(63), the repulsive part of the potential will be more relaxed by taking into account the last term in Eq.(63), the charge dipole interaction, in the range where the repulsive potential is effective.

4.3 Polarization and dielectric constant

To discuss the screened inter ionic potential by the dielectric function, we will briefly summarize the relation between the polarization and the dielectric constant. Suppose that the local electric field at the position of the ion is E_{loc}, the contribution to the polarizability is ordinary classified to the following three types; (*a*) the electron distribution change of the atomic core which occurs inside the ion. It has been discussed in the previous sections; (*b*) the contribution from ions, which occurs from the relative configuration of other neighbouring ions; (*c*) if the ion has the permanent electric dipole, its contribution should be considered, especially in the case that the ion consists of plural atoms. However, it is unnecessary to be taken into account in the case of molten alkali chloride or molten carbonate.

In the solid phase, if the frequency analysis is applied to the local electric field E_{loc}, (c) vanishes at about the micro wave length; next (*b*) disappears at the infrared region; (*a*) lasts to the end. In this discussion, we pay attention to (*a*) and (*b*).

According to the linear response theory, the relation between the electron polarizability discussed in the previous sections and the dielectric constant corresponding to it is expressed as,

$$1 - (1 / \varepsilon(q)) = 4p\alpha(q) \qquad (64)$$

Therefore, it is possible to obtain the effective inter ionic potentials in molten salts by the calculation of the term (*a*) and (*b*) using the polarization or the dielectric constant.

4.4 Our final form of inter-ionic potentials in molten salts

The dielectric function of the attractive part of the inter ionic potential of molten salts have been derived (Koishi et al., 2007; Matsunaga et al. 2007, 2008), and the theory have been extended to the polarizable model (Matsunaga and Tamaki, 2011). We briefly describe the procedure as follows. The Fourier component of the Coulomb potential in $\varphi_{ij}^0(r)$, i.e. $FT[z_i z_j e^2/r] = 4\pi z_i z_j e^2/q^2$ is screened by the dielectric function, as,

$$\{\text{the FT result of the screened Coulomb term in } \varphi_{ij}^{\ 0}(r)\} = 4\pi z_i z_j e^2/q^2\varepsilon(q) \quad (65)$$

As will be described in the next section, $\varepsilon(q)$ is related to the charge-charge structure factor $Szz(q)$. In other words, $\varepsilon(q)$ is introduced to the pair potential as, so to say, a factor of the many body effect, or the environmental factor. Adding the repulsive term ($\zeta H_{ij}/r^n$) and the dipole-dipole interaction term ($-\xi C_{ij}/r^6$) in $\varphi_{ij}^0(r)$ with the simplified reduction constants ζ and ξ to (65), the promise inter-ionic potentials in *a-b* binary molten salt screened by the many-body force are expressed as,

$$\varphi_{ij}(r) \equiv Inv.FT[4\pi z_i z_j e^2/q^2 e(q)] + \zeta H_{ij}/r^n - (1/2)\{1 - f_{ij}(r)\}^2(\alpha_i z_j e^2 + \alpha_j z_i e^2)/$$
$$/r^4 - \xi C_{ij}/r^6 \qquad (i, j = a, b) \quad (66)$$

where Inv.FT means the inverse Fourier transformation. The repulsive term in (66) can be replaced by the exponentially decaying functions.

Provided that the following function Eq.(67) is adopted as the decaying factor $f_{ab}(r)$, the desirable condition will be satisfied; as r approaches to 0, then $f_{ab}(r)$ approaches to 1; as r increases, then $f_{ab}(r)$ approaches to 0.

$$f_{ab}(r) = 2/\{\exp(+k_{ab}r) + \exp(-k_{ab}r)\} \quad (67)$$

where k_{ab} is a variable parameter, e.g. if $f_{+-}(r) \sim 0.2$ is required when the inter ionic distance is about 3 A, the estimated value is $k_{+-} \sim 0.77$ A^{-1}. Regarding $\varepsilon(q)$, the detailed discussion can been found in our previous works (Koishi et al., 2007; Matsunaga et al. 2007, 2008). As we have stated so far, the polarizable ion model in the short-range distance has been adopted in Eq.(66) where the repulsive potential (in both case $1/r^n$ function form and the exponentially decaying function) is dominant. On the other hand, the screening contribution is adopted in the long-range distance where the Coulomb attractive potential is dominant. Thus the plausible inter ionic potential can be obtained, as it was, the polarized and screened inter-ionic potentials model (PSIPM). We will demonstrate the example in the next section.

4.5 Application to molten CuI

In this section, we will show the example of application of the new theory to molten CuI. In molten CuI, the anomaly approach in Cu-Cu distribution is known, which is not reproduced by the classical MD (Waseda et al., 2000). Firstly, the outline of the theory of

the dielectric screening that we have developed in the previous section is briefly described as follows for the readers' benefit (Koishi et al., 2007; Matsunaga et al. 2007, 2008). As stated before, the Coulomb potential is screened by the dielectric constant $1/\varepsilon(q)$. $\varepsilon(q)$ is expressed using the charge-charge structure factor, $S_{ZZ}(q)$, which is defined as follows (Hansen and McDonald, 1986),

$$S_{zz}(q) = <r_q^{\ z} r_{-q}^{\ z}> /N = \Sigma_i \Sigma_j z_i z_j S_{ij}(q) \tag{68}$$

where z_i and z_j are the effective charge of ions. $S_{ij}(q)$ is the partial structure factor, i.e. the Fourier transformation of the pair distribution function of ion i and j, $g_{ij}(r)$, which is expressed as follows,

$$S_{ij}(q) = x_i \delta_{ij} + n x_i x_j \int_0^\infty (\sin qr/qr)\{g_{ij}(r) - 1\} 4\pi r^2 dr \tag{69}$$

The relation between $1/\varepsilon(q)$ and $S_{ZZ}(q)$ is expressed as,

$$\frac{1}{\varepsilon(q)} = \frac{1}{1 + \delta(\kappa^2/q^2) S_{zz}(q)} \tag{70}$$

where $\kappa_s^2 = 4\pi e^2 \beta n$, $\beta = 1/k_B T$, and n is the number density of constituent ions. The parameter δ is introduced to reduce the screening effect by the structure anisotropy as seen in molten noble metal halide. The value of δ is supposed to be in the range of $0 < \delta \le 1$. The condition $\delta = 1$ may occur in a well-symmetric configuration like molten alkali halide. In the region of high values of $q > 10A^{-1}$, $S_{ZZ}(q) \cong 1$ is valid, hence Eq.(70) will be written as,

$$\frac{1}{\varepsilon_i(q)} = \frac{1}{1 + \delta(\kappa^2/q^2)} \tag{71}$$

As we have describes in the previous section, the screened potentials can be obtained using $\varepsilon(q)$. In our previous work, to confirm the validity of the obtained potential, we have calculated the pair distribution function by the potential mean force (Hansen and McDonald, 1986), which is expressed as,

$$g_{ij}(r) = exp[-U^{ij}(r)/k_B T] \tag{72}$$

However, the screened potential $\varphi_{ij}(r)$ with the small reduction parameters multiplied on the repulsive term was used for $U^{ij}(r)$, and the calculation was restricted to the cation and anion pair.

On this stage, we try to make a slight modification of the interpretation of the theory. We consider two types of screened potentials; the first one, $\varphi_{ij}^S(r)$, is the screened potential that we have discussed in the previous section, which is affected by the structure through $S_{ZZ}(q)$; the second one, $\varphi_{ij}^I(r)$, is so to say, the 'ideal' screened potential with $\varepsilon_i(q)$ in Eq.(71), which expresses the effect from the uniform back ground. The potentials are written as,

$$\varphi_{ij}^{\ S}(r) \equiv Inv.FT[4\pi z_i z_j e^2 / q^2 \varepsilon(q)] + \zeta^S H_{ij} / r^n - (1/2)\{1 - f_{ij}(r)\}^2 (\alpha_i z_j e^2 + \alpha_j z_i e^2) / / r^4 - \xi^S C_{ij} / r^6 \qquad (i,j = a, b) \tag{73}$$

$$\varphi_{ij}^{\ I}(r) \equiv \text{Inv.FT}[4\pi z_i z_j e^2 / q^2 \varepsilon_i(q)] + \zeta^I H_{ij} / r^n - (1/2)(\alpha_i z_j e^2 + \alpha_j z_i e^2) /$$
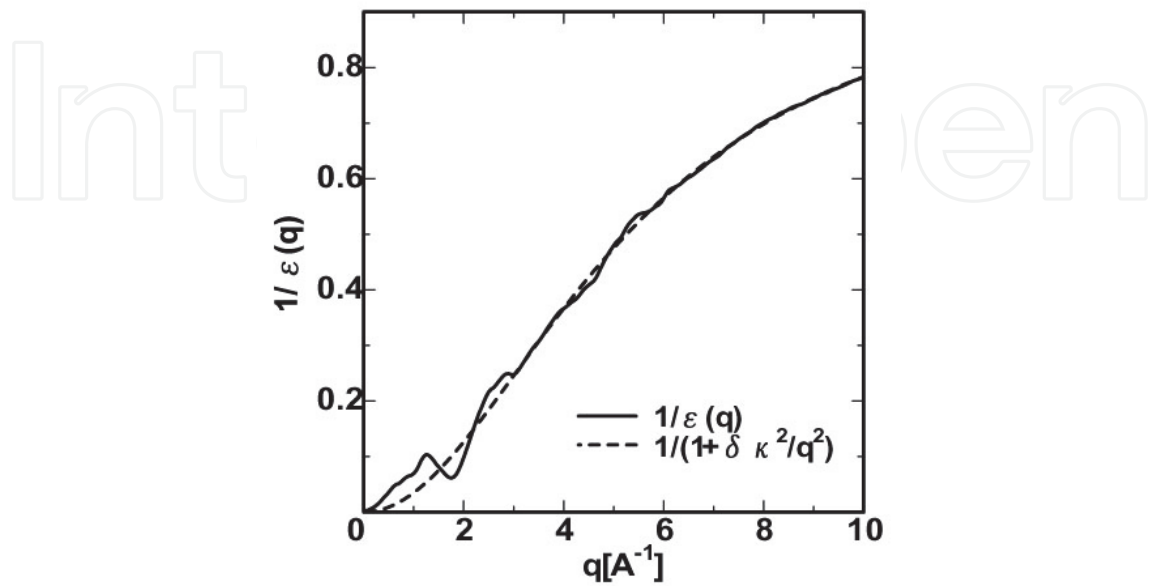$$/r^4 - \xi^I C_{ij} / r^6 \qquad (i,j = a, b) \tag{74}$$

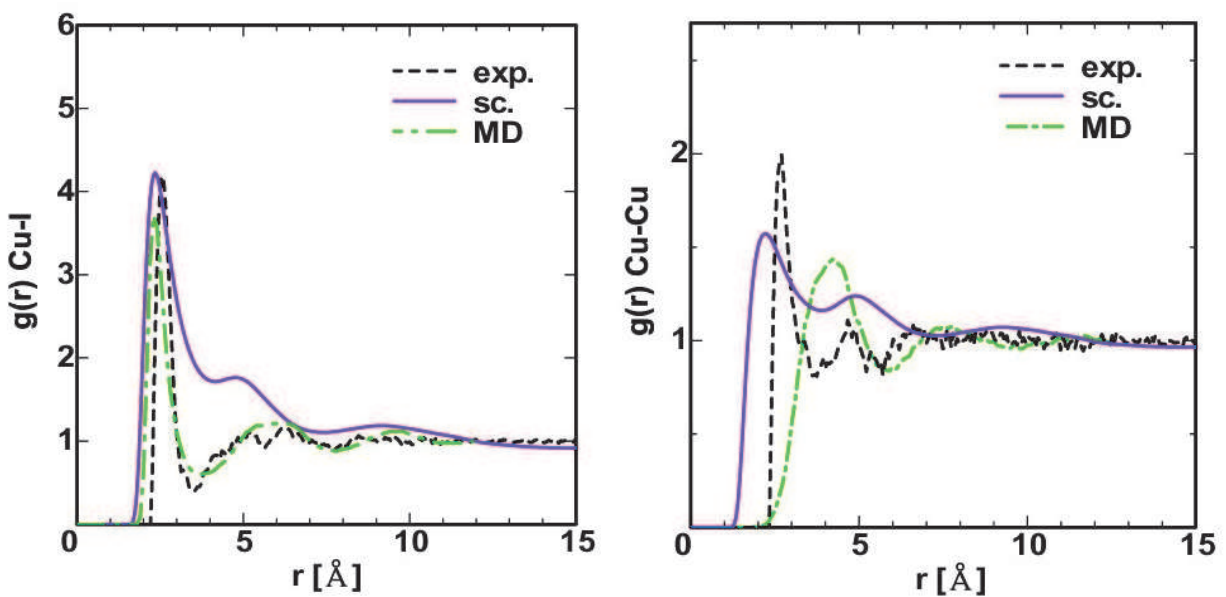Fig. 11. $1/\varepsilon(q)$ of molten CuI with $1/(1+\delta(\kappa_s^2/q^2))$.

Fig. 12. $g_{CuI}(r)$ (left) and $g_{CuCu}(r)$ (right) calculated using the screened potential with that obtained by experiment and by MD.

We take $U^{ij}(r)$ for the potential of mean force in Eq.(72) as the deviation from the ideal screening, as,

$$U^{ij}(r) \equiv -\Delta\varphi_{ij}(r) = -|\varphi_{ij}^{S}(r) - \varphi_{ij}^{I}(r)| \tag{75}$$

This interpretation seems to be appropriate because the effective mean force is originally defined for the weak interaction between particles, which corresponds to $\Delta\varphi_{ij}(r)$ in this case. In the numerical calculation, we adopt the value of δ in Eq.(70) and Eq.(71) as 0.4, $\Delta\zeta = |\zeta^S - \zeta^I| = 0.12$. C_{CuCu} and C_{CuI} are 0 in Eq.(73) and Eq.(74).

The obtained $g_{+-}(r)$ and $g_{++}(r)$ are shown in Fig.12 with $g_{ij}(r)$ obtained by experiment (Waseda et al., 2000), and MD using the original VR type potentials (Stafford et al., 1990). The first peak of $g_{+-}(r)$ and the phase of oscillations almost agree well, though the second peak height is not satisfactory reproduced. The first peak position of $g_{++}(r)$ obtained by the experiment suggests the anomalous closer distribution of Cu ions, which has been reproduced by the screened potentials and the effective mean force to some extent, except their peak heights and the oscillation phase of the third peak. On the other hand, the first peak of $g_{++}(r)$ obtained by MD obviously disagrees with the experiment. The discrepancy between $g_{ij}(r)$ by the experiment and that obtained by the screened potential may be caused by several reasons, besides a margin of error in the Fourier transformation. One of the expected reasons is that the non-symmetric structure in solid phase remains in molten phase, which may obstruct the screening effect in molten phase. Despite these facts, however, it may be suggested that the treatment described so far is physically significant, and the screening effect has the obvious contribution to the obtained results.
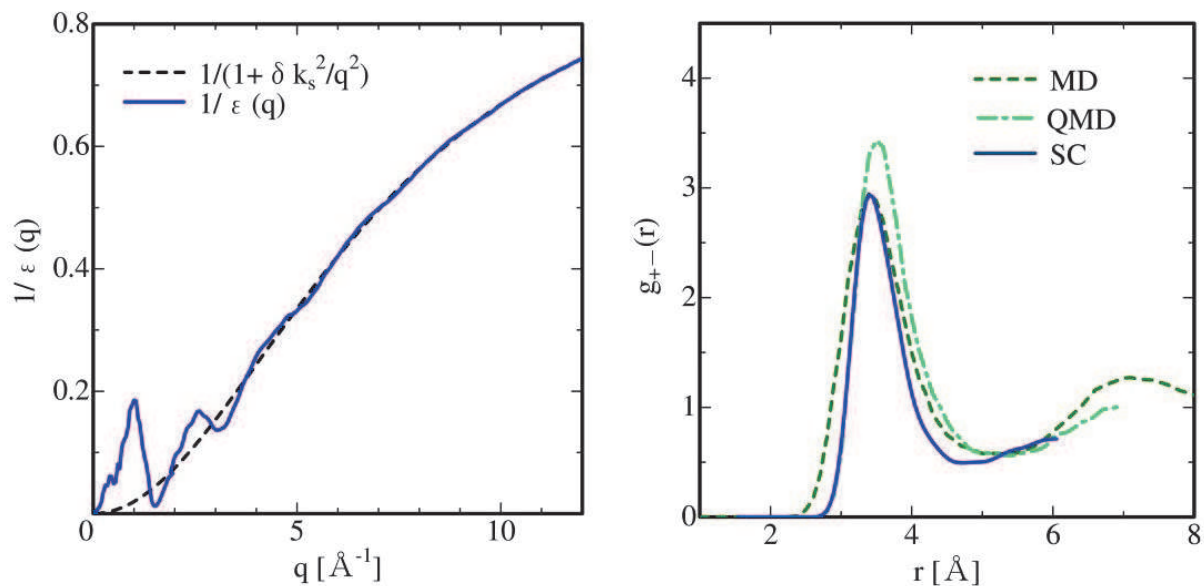

Fig. 13. $1/\varepsilon(q)$ of molten CsAu with $1/(1+\delta(\kappa_s^2/q^2))$ (left). $g_{+-}(r)$ calucaed using the screened potential with that obtained by MD and QMD.

4.6 Application to molten CsAu

Finally, we wish to show the application to molten CsAu system. Molten CsAu is a typical example which exibits a transition from a metallic to non-metallic state around a stoichiometric composition in molten phase, though both components are metallic conductors. Molten CsAu at the equiatomic composition exhibits a very low conductivity like molten salts (Schmutzler et al., 1976). These characteristics have been interpreted that a chemical short range order in the molten state are formed, in other words the molten CsAu alloy is composed of Cs^+ and Au^-. Structural measurements for molten CsAu systems using the neutron diffraction were performed (Marchin et al., 1980). Molten CsAu alloys have some structural characteristics of the short range order indicating a typical ionic compound. But partial structure factors have not yet been obtained experimentally.

Many attempts have been made to investigate the three dimensional configurations of the molten CsAu alloys by considering the partial structure factors and the pair distribution functions. The charged hard sphere model with the mean spherical approximation is mainly used for this purpose (Evans & Telo da Gama,1980; Holzhey et al., 1982). Hoshino indicated that the partial structure factors and the entropy of mixing depend strongly on the amount of charge transfer (K. Hoshino, 1984). Both of their consequences showed that the partial structure factors and the pair distribution functions of molten CsAu alloy have the same characteristics as those observed in molten alkali halides. However, the pair distribution functions obtained by the Monte Carlo simulation are very different from those obtained by the charged hard sphere model; Au^- - Au^- distance indicates the most closest approach (Costa Cabral et al., 1992). In this situation, we performed molecular dynamics simulation using the Tosi-Fumi type potentials to examine the structural and transport properties in molten CsAu (Matsunaga, 2000, 2001). The obtained structure of molten CsAu shows the similar characteristics to CsCl structure. On the other hand, the recent *ab initio* calculation in molten CsAu shows the good agreement in the pair distribution function of Cs-Au, $g_{CsAu}(r)$, with the molecular dynamics result, however there are discrepancies in $g_{AuAu}(r)$ and $g_{CsCs}(r)$ (Charpentier and Clérouin, 2008). This result may suggest the existence of the anomalous inter-ionic interactions in molten CsAu like molten CuI. This fact prompts us to examine the dielectric screening effect in molten AuCs. The calculation procedure is similar to that described before. The obtained calculation results are shown in Fig.13. It can be seen in Fig.13 that $g_{CsAu}(r)$s obtained by three different methods agrees well to some extent.

5. Conclusion

In this book chapter, we have re-examined the theory of the dielectric screening, and summarized the derivation of the new expression of the dielectric function. The extension of the theory to the potential mean force, and the deviation from the Nernst-Einstein relation has also been discussed. Then, we have reviewed the application studies of the new theory to the binary and ternary molten salts, i.e. alkali halides NaCl, RbBr, noble metal halides AgBr, CuBr, and AgBr-AgI mixture. The concentration-concentration fluctuation for the multi-component systems $S_{CiCj}(q)$ (Bhatia & Ratti, 1977) has also been discussed in relation with the many body effect and the short range order. We have applied the theory to the poralizable ion model. The new expression of the potential

which enables to avoide the polarization catastrophe has been proposed. The model has been applied to molten CuI and CsAu systems.

6. Acknowledgment

7. References

Berne, B. & Rice, S. A. (1964). On the Kinetic Theory of Dense Fluids. XVI. The Ideal Ionic Melt. *Journal of Chemical Physics.,Vol.* 40, Issue 5, (March 1964), pp. 1347-1362; DOI:10.1063/1.1725318

Bhatia, A. B. & Ratti, V. K. (1977). Number-Concentration structure factors and their long wavelength limit in multicomponent fluid mixtures. *Physics and Chemistry of Liquids*, Vol.6, Issue 3, (1977), pp.201-213, DOI:10.1080/00319107708084140

Bhatia, A. B. & Thornton, D. E. (1970). Structural Aspect of the Electrical Resistivity of Binary Alloys. *Physical Review B*, Vol.2, (October 1970), pp.3004-3012, DOI:10.1103/PhysRevB.2.3004

Bitrián, V. & Trullàs, J. (2006). Molecular Dynamics Study of Polarizable Ion Models for Molten AgBr. *Journal of Physical Chemistry*, Vol.110, Issue 14 (2006) pp.7490–7499, DOI: 10.1021/jp056818u

Chandra, S. (1981). *Superionic Solids: Principles and Applications*, Elsevier Science Ltd, ISBN: 0444860398, Amsterdam

Charpentier, N. & Clérouin, J. (2008). *Ab initio* simulations of the liquid alloy Au-Cs. Physical Review B, Vol.78, Issue 10, (September 2008), pp.100202-1-100202-2, DOI:10.1103/PhysRevB.78.100202

Costa Cabral, B. J.; Natalia, M.; Cordeiro, D. S. & Telo da Gama, M. M. (1991). The structure of molten CsAu: ab initio and Monte Carlo study. *Journal of Physics: Condensed Matter*, Vol.3, No.29, (July 1991), pp.5615-5620, DOI:10.1088/0953-8984/3/29/014

Edwards, F. G.; Enderby, J. E.; Howe, R. A. & Page, D. I. (1975). The structure of molten sodium chloride. *Journal of Physics C: Solid State Physic*, Vol.8, No.21, (November 1975), pp.3483-3490, DOI:10.1088/0022-3719/8/21/018

Endo, K.; Ida, T.; Kimura, J.; Mizuno, M.; Suhara, M. & Kihara, K. (1999). Structural analysis of $Ag_xCu_{1-x}I$ (0.75⩽x<1.00) in the superionic phase using solid NMR and X-ray diffraction methods. *Chemical Physics Letters*, Vol.308, Issues 5-6, (July 1999), pp.390-396, DOI:10.1016/S0009-2614(99)00631-4

Evans, R. &Telo Da Gama, M. M. (1980). Structural evidence that molten CsAu is ionic. *Philosophical Magazine Part B*, Vol.41, Issue 3, (1980), pp.351-356, DOI:10.1080/13642818008245391

Gartrell-mills, P. R. & McGreevy, R. L. (1989). Monte-Carlo Simulation of Molten CsCl Using a 'Deformation Dipole' Polarisable Ion Potential. *Molecular Simulation,*Vol.2, Issue 3, (1989), pp. 209-216, DOI:10.1080/08927028908031369

Hansen, J.P. &McDonald, I.R. (1986). *Theory of Simple Liquids* 2nd ed, Academic Press, New York.

Holzhey, C.; Brouers, F.; Franz, J. R. & Schirmacher,W. (1982). The theory of metal-non-metal transitions in gold alkali liquid alloys. *Journal of Physics F: Metal Physics*, Vol.12, No.11, (November 1982), pp.2601-2610, DOI:10.1088/0305-4608/12/11/018

Kittel, C. (1996) *Introduction to Solid State Physics 7th Edition*, John Wiley & Sons, Inc., New York, ISBN: 9780471111818

Koishi, T. & Tamaki, S. (2005). A theory of transport properties in molten salts. *Journal of Chemical Physics.* Vol.123, Issue 19, (November 2005), pp.194501-1 - 194501-11, DOI: 10.1063/1.2102901

Koishi, T.; Saito, M.; Matsunaga, S. & Tamaki, S. (2007). Dielectric screening properties in molten salts. *Phys. Chem. Liq.* Vol.45, No.2, (April 2007), pp.181-196, ISSN 0031-9104

Locke, J.; Messoloras, S.; Stewart, R. J.; McGreevy, R. L. & Mitchell, E. W. J. (1985). The structure of molten CsCl. *Philosophical Magazine Part B,*Vol.51, Issue 3, (1985), pp. 301-315, DOI:10.1080/13642818508240576

March, N.H. & Tosi, M. P. (1976). *Atomic Dynamics in Liquids*. Macmillan, London, ISBN: 0333112784

Martin, W.; Freyland, W.; Lamparter, P. & Steeb, S. (1980). Structure and Density of Gold-Cesium-Melts. II. Neutron Diffraction with Molten Gold-Cesium-alloys. *Physics and Chemistry of Liquids*, Vol.10, Issue 1, (1980), pp. 61-76, DOI:10.1080/003191080008078457

Matsunaga, S.; Ishiguro, T. & Tamaki, S. (1983). Thermodynamic properties of liquid Na-Pb alloys. *Journal of Physics F: Metal Physics*, Vol.13, No.3, (March 1983), pp.587-596, DOI:10.1088/0305-4608/13/3/009

Matsunaga, S. (2000). Structural Study on Liquid Au–Cs Alloys by Computer Simulations. *Journal of the Physical Society of Japan*, Vol.69, No.6, (June 2000), pp.1712-1716, DOI: 10.1143/JPSJ.69.1712

Matsunaga, S. (2001). Transport Properties in Liquid AuCs Alloy. *Journal of the Physical Society of Japan*, Vol.70, No.12, (December 2001) pp.3591-3595, DOI: 10.1143/JPSJ.70.3591

Matsunaga, S. (2003). Structural Properties in Ag3SI: A Molecular Dynamics Study of Superionic and Molten Phases. *Journal of the Physical Society of Japan*, Vol.72, No.6, (June 2003), pp.1396-1402, DOI: 10.1143/JPSJ.72.1396

Matsunaga, S. & Madden, P.A. (2004). Structural and transport properties in the Ag3SI system: a molecular dynamics study of alpha, beta and molten phases. *Journal of Physics: Condensed Matter*, Vol.16, (January 2004), pp. 181-194, DOI:10.1088/0953-8984/16/3/001

Matsunaga, S. (2005). Structural and transport influence of dissolving AgBr into AgI in super ionic and molten phases by molecular dynamics simulations. *Solid State Ionics*, Vol.176, Issues 23-24, (July 2005), pp.1929-1940, DOI:10.1016/j.ssi.2005.04.045

Matsunaga, S.; Saito, M.; Koishi, T. & Tamaki, S. (2007). Dielectric screening effects in molten AgI-AgBr system. *Molecular Simulation*, Vol.33, Nos 1-2, (January–February 2007), pp.153-158, ISSN 0892-7022

Matsunaga, S.; Saito, M.; Koishi, T. & Tamaki, S. (2008). Dielectric screening properties in molten noble-metal halides. *Journal of Alloys and Compounds*, Vol.452, (March 2008), pp.182-187, DOI:10.1016/j.jallcom.2006.12.161

Matsunaga, S. & Tamaki, S. (2008). Premelting phenomena in ionic crystals. *Journal of Physics: Condensed Matter*, Vol.20, No.11, (March 2008), pp.114116-1-114116-9, DOI:10.1088/0953-8984/20/11/114116

Matsunaga, S. & Tamaki, S. (2008). Hetero-phase fluctuations in the pre-melting region in ionic crystals. *The European Physical Journal B*, Vol.63, No.4, (June 2008), pp.417-424, DOI: 10.1140/epjb/e2008-00245-3

Matsunaga, S. (2009). Structural features of superionic phase in AgBr-CuBr system by molecular dynamics simulation. *Journal of Physics: Conference Series*, Vol.144, No.1, (January 2009), pp.012011-1-012011-4, DOI:10.1088/1742-6596/144/1/012011

Matsunaga, S. (2009). Structure and Atomic Dynamics of Silver Halide Mixtures. *Progress of Theoretical Physics Supplement*, No. 178 (2009) pp. 113-119, DOI:10.1143/PTPS.178.113

Matsunaga, S. & Tamaki, S. (2011). On the inter ionic potentials. *EPI Web of Conferences*, (May 2011), Vol.15, pp.02010-p.1 -02010-p.6, DOI: 10.1051/epjconf/20111502010

Parrinello, M.; Rahman, A. & Vashishta, P. (1983). Structural Transitions in Superionic Conductors. *Physical Review Letters*, Vol.50, Issue 14, (April 1983), pp.1073–1076, DOI:10.1103/PhysRevLett.50.1073

Saito, M.; Park, C.; Omote, K.; Sugiyama K. & Waseda Y. (1997). Partial Structural Functions of Molten CuBr Estimated from the Anomalous X-Ray Scattering Measurements. *Journal of the Physical Society of Japan*, Vol.66, No. 3, (March 1997), pp. 633-640, DOI: 10.1143/JPSJ.66.633

Saito, M.; Kang, S.; Sugiyama, K. & Waseda, Y. (1999). Partial Structural Functions of Molten AgBr Estimated from the Anomalous X-Ray Scattering Data Coupled with Neutron Diffraction. *Journal of the Physical Society of Japan*, Vol.68, No.6, (June 1999), pp. 1932–1938, ISSN 0031-9015

Schmutzler, R. W.; Hoshino, H.; Fischer, R. & Hensel, F. (1976). Nonelectronic Electrical Transport in Liquid CsAu. *Berichte der Bunsengesellschaft für Physikalische Chemie*, Vol.80, Issue 2, (February 1976), pp.107–113, DOI: 10.1002/bbpc.19760800203

Stafford, A. J.; Silbert, M.; Trullàs, J. & Giró, A. (1990). Potentials and correlation functions for the copper halide and silver iodide melts. I. Static correlations. *Journal of Physics: Condensed Matter*, Vol.2, No.31, (August 1990), pp.6631-6642, DOI:10.1088/0953-8984/2/31/016

Tasseven, Ç.; Trullàs, J.; Alcaraz, O.; Silbert, M. & Giró, A. (1997). Static structure and ionic transport in molten AgBr and AgCl. *Journal of Chemical Physics.* Vol. 106, Issue 17, (May 1997), pp.7286-7294 , doi:10.1063/1.473690

Vashishta, P. & Rahman, A. (1978). Ionic Motion in α-AgI. *Physical Review Letters*, Vol.40, Issue 20, (May 1978), pp. 1337–1340, DOI:10.1103/PhysRevLett.40.1337

Waseda, Y.; Kang, S.; Sugiyama, K.; Kimura, M. & Saito, M. (2000). Partial structural functions of molten copper halides CuX (X = Br, I) estimated from the anomalous x-ray scattering measurements. *Journal of Physics: Condensed Matter*, Vol.12, (February 2000), A195-A202, DOI:10.1088/0953-8984/12/8A/323

Wilson, M.; Madden, P. A. & Costa-Cabral, B. J. (1996). Quadrupole Polarization in Simulations of Ionic Systems: Application to AgCl. *the Journal of Physical Chemistry*, Vol.100, Issue 4, (January 1996), pp 1227–1237, DOI: 10.1021/jp9512319
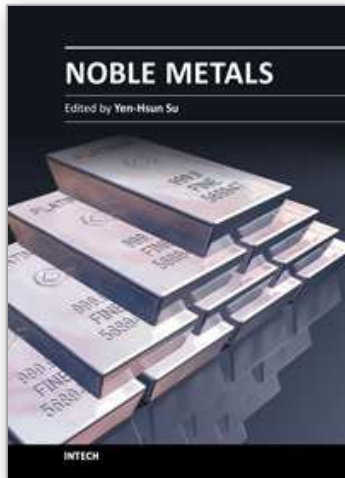
Noble Metals

Edited by Dr. Yen-Hsun Su

This book provides a broad spectrum of insights into the optical principle, resource, fabrication, nanoscience, and nanotechnology of noble metal. It also looks at the advanced implementation of noble metal in the field of nanoscale materials, catalysts and biosystem. This book is ideal not only for scientific researchers but also as a reference for professionals in material science, engineering, nonascience and plasmonics.

How to reference

In order to correctly reference this scholarly work, feel free to copy and paste the following:

Shigeki Matsunaga, Takahiro Koishi, Masatoshi Saito and Shigeru Tamaki (2012). Dielectric Screening Properties and Many Body Effects in Molten Salts, Noble Metals, Dr. Yen-Hsun Su (Ed.), ISBN: 978-953-307-898-4, InTech, Available from: http://www.intechopen.com/books/noble-metals/dielectric-screening-properties-and-many-body-effects-in-molten-salts

INTECH
open science | open minds